Landau theory of tilting of oxygen octahedra in perovskites

A. B. Harris*

Department of Physics and Astronomy, University of Pennsylvania, Philadelphia, Pennsylvania 19104, USA

(Received 13 June 2011; published 18 May 2012)

The list of possible commensurate phases obtained from the parent tetragonal phase of Ruddlesden-Popper (RP) systems, $A_{n+1}B_nC_{3n+1}$ for general n due to a single phase transition involving the reorienting of octahedra of C (oxygen) ions is reexamined using a Landau expansion. This expansion allows for the nonlinearity of the octahedral rotations and the rotation-strain coupling. It is found that most structures allowed by symmetry are inconsistent with the constraint of rigid octahedra, which dictates the form of the quartic terms in the Landau free energy. For A_2BC_4 our analysis allows only 10 of the 41 structures which satisfy the general symmetry arguments of Hatch *et al.* [Phys. Rev. B **39**, 9282 (1989)]. The symmetry of rotations for RP systems with $n > 2$ is clarified. Our list of possible structures for general n excludes many structures allowed in previous studies.

DOI: 10.1103/PhysRevB.85.174107 PACS number(s): 61.50.Ks, 61.66.−f, 63.20.−e, 76.50.+g

I. INTRODUCTION

The Ruddlesden-Popper (RP) compounds[1] are layered perovskites having the chemical formula $A_{n+1}B_nC_{3n+1}$ and which consist of two slabs of BC_6 octahedra per conventional unit cell. Each slab consists of n layers of corner sharing octahedra of C ions, where C is usually either fluorine or oxygen. These systems either are or can be considered to be developed via one or more structural transitions from the high-symmetry tetragonal parent structure shown in Fig. 1 for the cases exemplified by K_2MgF_4 ($n = 1$) and $Ca_3Mn_2O_7$ ($n = 2$). We refer to the RP system with $n = 1$ as RP214 and to that with $n = 2$ as RP327.

The RP systems exhibit many interesting technological properties such as high-T_c superconductivity,[2] colossal magnetoresistance,[3] metal insulator transitions,[4] and coupled ferroelectric and magnetic order.[5–7] Many of these properties depend sensitively on the distortions from the ideal tetragonal $I4/mmm$ structure (see Fig. 1) of space group 139 which appear at structural phase transitions.[8–12] (Numbering of space groups is from Ref. 13.) Accordingly, an accurate characterization of their structure is essential to reach a detailed understanding of their properties. Such an understanding can potentially lead to the fabrication of new systems with enhanced desired properties. It is therefore not surprising that one of the most celebrated theoretical problems in crystallography is to list the possible structures that can result from a single structural phase transition in which the (usually oxygen) interlocking octahedra are cooperatively reoriented under the constraint that they are distorted only weakly (in a sense made precise below). One of the earliest works to address this question was that of Glazer,[14] who analyzed possible structural distortion from the cubic parent structure of $CaTiO_3$. It turned out that a few of the structures he found did not actually satisfy the constraint of not distorting the octahedra.[15] For the RP214 systems the two principal approaches to this problem which have been used are (a) a direct enumeration of likely structures[16] and (b) the use symmetry.[17] The second approach utilizes a very useful computer program[18] to generate the isotropy subgroups of Ref. 19. In this way Hatch *et al.*[17] gave a listing for the RP214 structure of possible phase transitions involving distortions at various high symmetry wave vectors. This listing was shown to be consistent with the revised results of method (a).[17] This important work has stood unquestioned for over a decade.[20] Here we show that most of structures listed in Refs. 17, 20, and 21 for the RP214 systems are inconsistent with the constraint of rigid octahedra. To implement this constraint, we assume that the spring constants for distortion of the octahedra are larger than the other spring constants of the lattice by a factor of λ. Most of our results are obtained to leading order in $1/\lambda$, which we regard as an expansion parameter. This constraint causes the quartic terms in the Landau free energy to assume a form which is less general than allowed by symmetry. In some cases this constraint causes us to reject structures which simultaneously have distorted and undistorted sublattices, a situation which is counterintuitive, since it is analogous to a magnetic system simultaneously having ordered and disordered sublattices. Even for structures which our analysis allows, it is inevitable that in the structural phase transition the octahedra will undergo small (of order $1/\lambda$) distortions, which are observed.[22] In Glazer's work[14] this constraint was taken into account by constructing a flexible model of interlocking tetrahedra.[23] Here this constraint is treated analytically within the Landau expansion.

Briefly, this paper is organized as follows. In Sec. II we enumerate the high-symmetry wave vectors of the distortions we consider and we discuss the role of the quartic terms in the Landau expansion in determining the detailed nature of the distortions. Here we also develop the nonlinear constraint induced by the rigidity of the octahedra. In Sec. III we apply these ideas to enumerate the possible structures which are allowed via a single phase transition involving a distortion at these high-symmetry wave vectors for the RP214 structure. Our results are summarized in Tables II and III, below. In Sec. IV we extend the treatment to the analogous RP327 ($A_3B_2C_7$) bilayer system. In Sec. V we use our results for $n = 1$ and $n = 2$ RP systems to obtain results for the RP systems $A_{n+1}B_nC_{3n+1}$ consisting of n-layer slabs (with n finite). Our results for general n are given in Table VII, below. In Sec. VI we discuss and summarize our results. In this paper we include the coupling of octahedral reorientations to uniform strains and in an appendix we discuss how thermal fluctuations remove some unphysical apsects of the mean-field elastic response to octahedral reorientations. A brief report[24] in which the coupling to strains was omitted gave results similar to those given here. In a future paper we will consider phases which can be reached via two or more successive phase transitions.[6,17]

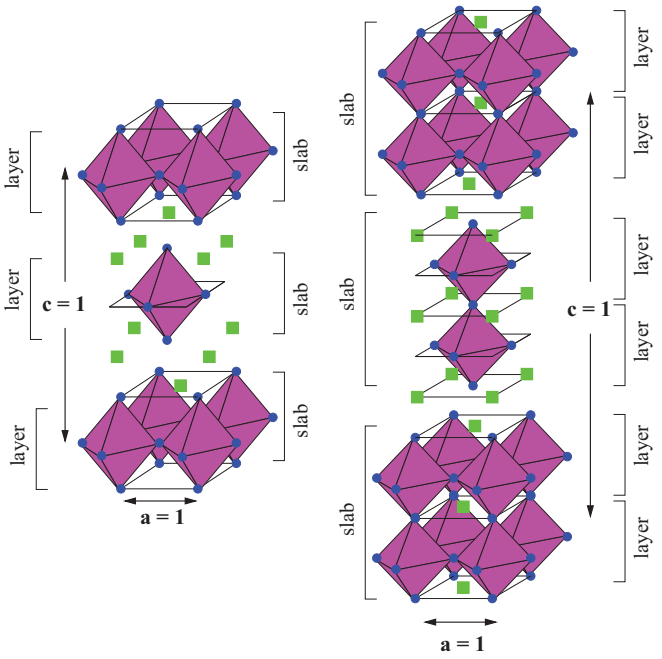

FIG. 1. (Color online) The high-symmetry (body-centered tetragonal) parent structure of A_2BO_4 (left) and $A_3B_2O_7$ (right). The green squares are A ions. The B ions are at the centers of the oxygen (blue dots) octahedra. We indicate what we call "layers" and "slabs." For $A_{n+1}B_nC_{3n+1}$ each slab contains n layers. The lattice constants a and c, which define the unit cell, are indicated.

II. GENERAL PRINCIPLES

A. Overview

We analyze possible distortions from the parent tetragonal system using a Landau-like formulation in which we write the free energy F (always per unit volume) as

$$F = \frac{1}{2}\sum_{k,l} A_{k,l}(T)X_kX_l + \mathcal{O}(X^4), \tag{1}$$

where X_k is a component of an ionic displacement. A structural phase transition occurs at a temperature T_0 when an eigenvalue of the matrix $\mathbf{A}$ becomes zero. (For $T > T_0$ all the eigenvalues of $\mathbf{A}$ are positive.) If the zero (critical) eigenvalue is N-fold degenerate, then for T near T_0 one has

$$F \sim \frac{a}{2}(T - T_0)\sum_{k=1}^{N} Q_k^2, \tag{2}$$

where Q_k is the amplitude of the kth linear combination of X's associated with the critical eigenvector of $\mathbf{A}$. As we shall see, higher-order (in Q) corrections to the free energy in the cases of interest involve only even powers of the Q's.

As is customary (e.g., see Ref. 17), we restrict attention to the cases when Q is a superposition of displacements associated with the star of the high-symmetry wave vectors $\mathbf{X} = (1/2,1/2,0)$, $\mathbf{N} = (1/2,0,1/2)$, or $\mathbf{P} = (1/2,1/2,1/2)$.[25] These vectors are on faces of the first Brillouin zone as shown in Fig. 2. The reciprocal lattice vectors are

$$\mathbf{G}_1 = (0,1,1), \qquad \mathbf{G}_2 = (1,0,1),$$
$$\mathbf{G}_3 = (1,1,0). \tag{3}$$

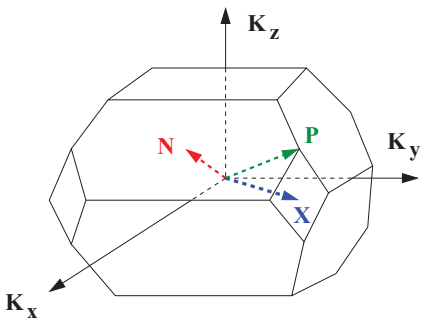

FIG. 2. (Color online) The first Brillouin zone for RP systems. There are two inequivalent $X = (1/2,1/2,0)$ points, four inequivalent **N** points, and two inequivalent **P** points. (Wave vectors are "equivalent" if their difference involves an integer number of reciprocal lattice vectors **G**.)

Instead of dealing with irreducible representations (irreps), we develop the free energy for the most general structure which can be constructed using the angular distortions at the wave vectors of the star of **X**, **N**, or **P**.

To see how the form of the fourth-order potential affects possible structural distortions, consider a system with two order parameters Q_1 and Q_2 related by symmetry, for which the free energy assumes the form

$$F = (T - T_0)\left[Q_1^2 + Q_2^2\right] + u\left[Q_1^2 + Q_2^2\right]^2 + vQ_1^2Q_2^2 \tag{4}$$

up to fourth order in Q with $u > 0$. As the temperature is lowered through the value T_0 the nature of the ordering depends on the sign of v. (See the phase diagram of Fig. 3.) If v is positive, then ordering has either Q_1 or Q_2 zero. If $-4u < v < 0$, ordering occurs with $|Q_1| = |Q_2|$. At the multicritical point[26,27] where v is zero (and also a similar sixth-order anisotropy vanishes) one can have ordering in an arbitrary direction of order parameter (Q_1-Q_2) space. However, we do not consider multicritical points because they require adjusting *two* control parameters such as the temperature *and*, say, the pressure or the electric field, etc. So the results of the present paper (as well as those of Refs. 17 and 20) should be interpreted as being relevant to phenomena which occur when only a single control parameter, such as the temperature, is varied. However, when u and v are small, one

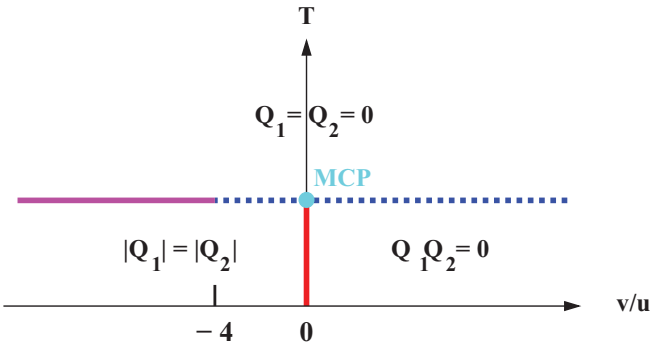

FIG. 3. (Color online) The mean-field phase diagram (Ref. 27) (schematic) for the free energy of Eq. (4), showing the multicritical point (MCP) at $v = 0$. The dashed line indicates a continuous phase transition and the solid line indicates a discontinuous one.

can have a weak first-order transition in which ordering can occur in an arbitrary direction in Q_1-Q_2 space. Note that if we invoke *only* the symmetry properties of the system, there is no constraint on the parameters u and v, in which case the analysis of Ref. 17 would apply. However, as we explain below, the picture of the lattice as consisting of interlocking oxygen octahedra implies a special form of the quartic terms with $u > 0$ and $v = -2u$, so that in most cases only structures with $|Q_1| = |Q_2|$ will actually occur.

B. Octahedral constraint

We now discuss the possible distorted configurations as constrained by the rigidity of the oxygen (or C ion) octahedra. In describing the distortions we use a notation similar to that of Refs. 17 and 20 which we deem more convenient for the quasiplanar RP systems than the widely used Glazer notation[14] for pseudocubic perovskites. For a single RP layer, we first consider the rotation of octahedra through an angle 2θ about the tetragonal axis. Giving the angle of rotation of one octahedron at the origin fixes the rotation angles of all other octahedra in this layer. In the Glazer notation this would be specified as $a^0a^0b^+$ or $a^0a^0b^-$, where the superscripts 0 indicate zero rotation about the axes x and y, and b (implicitly equal to 2θ) is the rotation angle about the third (z) axis. The superscript $+$ or $-$ on b tells how the angle varies as we move from one layer perpendicular to z to the next layer. Since for RP systems we have two slabs to consider, there would be two sets of Glazer symbols, one for each slab. Accordingly, for RP systems we introduce a notation similar to that of Refs. 17 and 20, which applies when the star of the wave vector is specified. (For the pseudocubic perovskites the Glazer symbol implicitly specifies the wave vector by the array of superscripts.)

For a rotation about the tetragonal z axis, the situation is that shown in Fig. 4. There one sees that a vertex common to two adjacent octahedra would, if the vertices were considered to be separate vertices for the two octahedra, become two closely, but distinct, separated points. In order to recover the common vertex, the two points would have to coalesce, which would require octahedral distortions of $\Delta_x/2$ and $\Delta_y/2$. However, it is possible for the lattice to relax, so that this mode would take place *without* any distortion of the octahedra. This relaxation involves macroscopic strains along the x and y axes, to account for the Δ displacements. For RP214 the octahedral distortions in the x-y plane are

$$\Delta_{x,n} = 2a\theta_n^2, \qquad \Delta_{y,n} = 2a\theta_n^2, \tag{5}$$

where $\Delta_{\alpha,n}$ is the value of Δ_α for the nth layer ($n = 1,2$) for the two layers in the RP214 system.

We need to generalize Eq. (5) to allow for the rotation of octahedra about the tetragonal x and y axes. In the seminal work of Ref. 14 we are reminded that the group of rotations is non-Abelian: Rotations about different axes do not commute with one another. Here we discuss a simple nonlinear treatment of small rotations. We define the orientation of an octahedron by three variables, θ, ϕ_x, and ϕ_y which correspond to small rotations about the tetragonal axes.[28] These three variables correspond to the three Euler angles needed to specify the orientation of a rigid body when the rotation from the undistorted state is small. This situation is somewhat similar to the spin wave expansion in which one introduces transverse spin components to describe the rotation of a three-dimensional spin. A simple way to deal with this situation is to express the orientation of the vectors from the center of the octahedron to the equatorial vertices in terms of their transverse displacements as

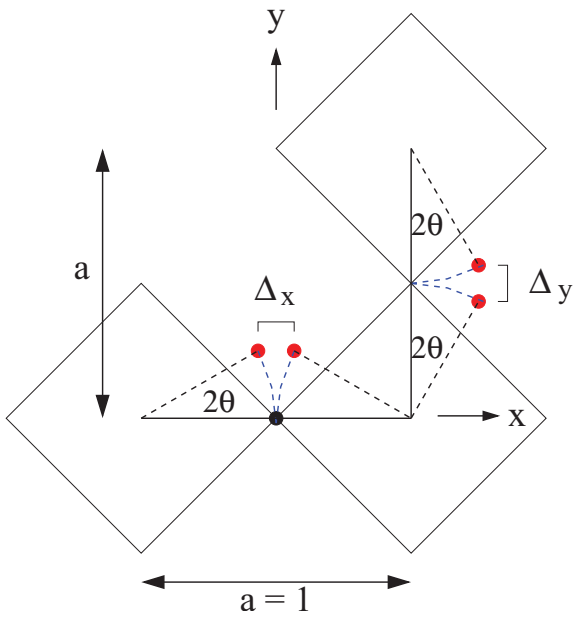

FIG. 4. (Color online) The octahedral constraint for interlocking θ rotations about the tetragonal z axis (which is perpendicular to the plane of the paper). The squares represent the cross sections of octahedra in an a-b plane. Here $\Delta_x = \Delta_y = 2a\theta^2$, where Δ_α is the mismatch that has to be absorbed either by a distortion of the octahedron or by a macroscopic strain when the octahedron is undistorted.

$$\begin{aligned}
\mathbf{r}_1 &= \left(\sqrt{1/4 - y_1^2 - z_1^2}, y_1, z_1\right),\\
\mathbf{r}_2 &= \left(x_2, \sqrt{1/4 - x_2^2 - z_2^2}, z_2\right),\\
\mathbf{r}_3 &= \left(-\sqrt{1/4 - y_3^2 - z_3^2}, y_3, z_3\right),\\
\mathbf{r}_4 &= \left(x_4, -\sqrt{1/4 - x_4^2 - z_4^2}, z_4\right),
\end{aligned} \tag{6}$$

where $\mathbf{r}_1$, $\mathbf{r}_2$, $\mathbf{r}_3$, and $\mathbf{r}_4$ are the rotated positions of the vertices whose respective original locations were (1/2,0,0), (0,1/2,0), (−1/2,0,0), and (0, − 1/2,0). Clearly, to retain the octahedral shape (with the center of mass fixed) we require that $\mathbf{r}_3 = -\mathbf{r}_1$ and $\mathbf{r}_4 = -\mathbf{r}_2$. We wish to incorporate the octahedral constraint to leading order in the transverse displacements. This constraint leads to

$$\begin{aligned}
|\mathbf{r}_1 \pm \mathbf{r}_2|^2 = \tfrac{1}{2} = &\left(x_2 \pm \sqrt{\tfrac{1}{4} - y_1^2 - z_1^2}\right)^2\\
&+ \left(y_1 \pm \sqrt{\tfrac{1}{4} - x_2^2 - z_2^2}\right)^2 + (z_1 \pm z_2)^2
\end{aligned} \tag{7}$$

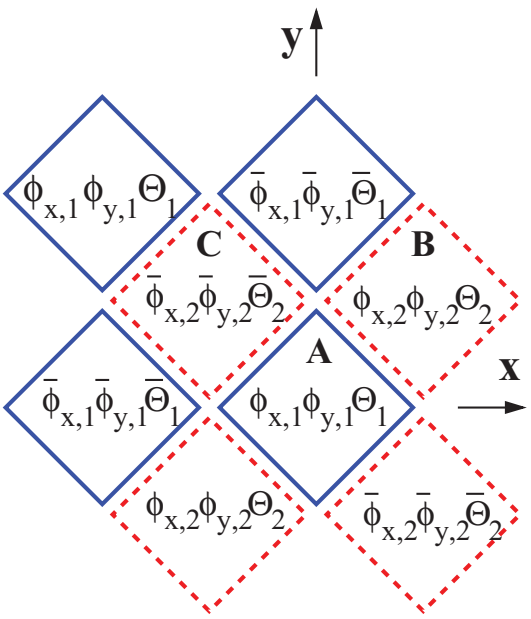

FIG. 5. (Color online) The structure of corner-sharing octahedra for the star of $\mathbf{X} \equiv (1/2,1/2,0)$ and $\mathbf{P} \equiv (1/2,1/2,1/2)$. The solid squares are the cross sections of octahedra in the $z = 0$ plane and the dashed squares are those in the $z = 1/2$ plane. For clarity the octahedra are slightly separated instead of sharing vertices. Here ϕ_x means that the $+x$ vertex moves up by an amount ϕ_x and the $-x$ vertex moves down by an amount ϕ_x and ϕ_y means that the $+y$ vertex moves up by an amount ϕ_y and the $-y$ vertex moves down by an amount ϕ_y. Also, 2θ is the angle of rotation about the z axis. Here and below $\overline{Q}$ denotes $-Q$. For $\mathbf{X}$ the structure is invariant under $z \to z + 1$. For $\mathbf{P}$ the variables change sign under $z \to z + 1$. The octahedral labels A, B, and C are needed for the discussion in the text.

so that

$$0 = x_2\sqrt{\tfrac{1}{4} - y_1^2 - z_1^2} + y_1\sqrt{\tfrac{1}{4} - x_2^2 - z_2^2} + z_1 z_2. \quad (8)$$

This gives

$$0 = x_2\left[\tfrac{1}{2} - y_1^2 - z_1^2\right] + y_1\left[\tfrac{1}{2} - x_2^2 - z_2^2\right] + z_1 z_2 + \mathcal{O}(q^5), \quad (9)$$

where q is one or more of the angular variables. Thus,

$$\frac{x_2 + y_1}{2} = -z_1 z_2 + x_2\left(y_1^2 + z_1^2\right) + y_1\left(x_2^2 + z_2^2\right) + \mathcal{O}(q^5). \quad (10)$$

We transform from the variables x_2 and y_1 to θ and $\delta\theta$:

$$x_2 = -\theta + \delta\theta, \qquad y_1 = \theta + \delta\theta, \quad (11)$$

so that

$$\delta\theta = -z_1 z_2 + [-\theta + \delta\theta]\left[(\theta + \delta\theta)^2 + z_1^2\right] + [\theta + \delta\theta]\left[(-\theta + \delta\theta)^2 + z_2^2\right] + \mathcal{O}(q^5), \quad (12)$$

which gives

$$\delta\theta = -z_1 z_2 + \theta\left(z_2^2 - z_1^2\right) + \mathcal{O}(q^4). \quad (13)$$

To make contact with the body of the paper (see Fig. 5, below), replace z_1 with ϕ_x and z_2 with ϕ_y to get

$$\begin{aligned} x_1 &= \tfrac{1}{2} - y_1^2 - z_1^2 = \tfrac{1}{2} - \phi_x^2 - \theta^2 + 2\theta\phi_x\phi_y + \mathcal{O}(q^4), \\ x_2 &= -\theta - \phi_x\phi_y + \theta\left(\phi_y^2 - \phi_x^2\right) + \mathcal{O}(q^4), \\ y_2 &= \tfrac{1}{2} - x_2^2 - z_2^2 = \tfrac{1}{2} - \phi_y^2 - \theta^2 - 2\theta\phi_x\phi_y + \mathcal{O}(q^4), \\ y_1 &= \theta - \phi_x\phi_y + \theta\left(\phi_y^2 - \phi_x^2\right) + \mathcal{O}(q^4). \end{aligned} \quad (14)$$

One sees that in terms of the variables θ, ϕ_x, and ϕ_y the actual positions of the vertices are given by power series expansion in these variables, the lowest term of which identifies these variables directly with the corresponding displacements. (Of course, this expansion is only useful if the variables are small.) We use these variables (which are essentially the three components of the angular momentum vector) to analyze the free energy. In calculating scattering cross sections one must, of course, use the actual positions of the ions given by their nonlinear expansion, such as that in Eq. (14) or in Fig. 6, below.

III. RP214 STRUCTURES

We start by considering the RP214 structures shown in the left panel of Fig. 1, so that each slab consists of a single layer.

A. The star of X

Here we will develop a Landau expansion for these structures which arise from distortions associated with the star of the wave vector, $\mathbf{X}$, which includes $\mathbf{X}_1 = (1/2,1/2,0)$ and $\mathbf{X}_2 \equiv (1/2, -1/2,0)$ providing that the octahedra rotate as constrained by their shared vertex (see Fig. 5). In the $z = 0$ plane both $\mathbf{X}_1$ and $\mathbf{X}_2$ each imply that all angular variables alternate in sign as one moves between nearest neighbors. This fact fixes the values of all the ϕ's and θ's in the $z = 0$ plane in terms of the values for the octahedron labeled A in Fig. 5. If we had only the wave vector $\mathbf{X}_1$, then the variables for octahedron B would be the negatives of those for octahedron A and the variables of octahedron C would be identical to those for octahedron A. If we had only the wave vector $\mathbf{X}_2$ then the variables for octahedra B and C would be reversed from what they were for wave vector $\mathbf{X}_1$. Thus, if we have a linear combination of the two wave vectors, the orientational state for the plane $z = 1/2$ is characterized by assigning arbitrary values to the variables of octahedron B relative to which the values of all the other variables in that plane are fixed. Thus, Fig. 5 gives the most general structure associated with the star of $\mathbf{X}$.

In Fig. 6 we identify the displacements of the vertices for the star of $\mathbf{X}$ using Eq. (14). From this figure we obtain the mismatch of the vertex when considered to be two independent vertices of adjacent octahedra to be

$$\begin{aligned} x_B - x_A &= 2\phi_x^2 + 2\theta^2 + \partial u_x/\partial x \\ &= 2\phi_x^2 + 2\theta^2 + \epsilon_{xx}, \\ y_B - y_A &= 2\phi_x\phi_y + \partial u_y/\partial x \\ &= 2\phi_x\phi_y + \epsilon_{xy}, \\ y_E - y_D &= 2\phi_y^2 + 2\theta^2 + \partial u_y/\partial y \\ &= 2\phi_y^2 + 2\theta^2 + \epsilon_{yy}, \end{aligned} \quad (15)$$

$$x_E - x_D = 2\phi_x\phi_y + \partial u_x/\partial y$$
$$= 2\phi_x\phi_y + \epsilon_{xy},$$

with corrections at order q^4. Here u_α is the α component of the displacement field and we have introduced the symmetric strain tensor, defined by

$$\epsilon_{\alpha\beta} = \frac{1}{2}\left[\frac{\partial u_\alpha}{\partial r_\beta} + \frac{\partial u_\beta}{\partial r_\alpha}\right]. \tag{16}$$

We have dropped contribution from the antisymmetric strain tensor (which corresponds to a rotation of the system).

The elastic free energy, $F_{\rm Oct}$, due to the deformation of the octahedra is proportional to the expansion parameter $\lambda \gg 1$. In terms of the variables of Fig. 6, $F_{\rm Oct}$ is constrained by symmetry to be of the form

$$F_{\rm Oct} = c_1\lambda[(x_B - x_A)^2 + (y_E - y_D)^2]$$
$$+ (c_2\lambda/2)[(y_B - y_A)^2 + (x_E - x_D)^2]$$
$$+ c_3\lambda[(y_B - y_A)(x_E - x_D) + (y_E - y_D)(x_B - x_A)]. \tag{17}$$

In writing this result we did not allow cross terms like $(x_B - x_A)(y_B - y_A)$, which are not invariant with respect to the mirror plane $(m_d\mathcal{R}_4)$ perpendicular to the x axis. Then, taking account of the two layers per unit cell, we have

$$F_{\rm Oct} = c_1\lambda\sum_{k=1}^{2}\left[\left(2\phi_{x,k}^2 + 2\theta_k^2 + \epsilon_{xx}\right)^2\right.$$
$$\left. + \left(2\phi_{y,k}^2 + 2\theta_k^2 + \epsilon_{yy}\right)^2\right]$$
$$+ c_2\lambda\sum_{k=1}^{2}[(2\phi_{x,k}\phi_{y,k} + \epsilon_{xy})^2]$$
$$+ c_3\lambda\sum_{k=1}^{2}\left[\left(2\phi_{x,k}^2 + 2\theta_k^2 + \epsilon_{xx}\right)\right.$$
$$\left.\times\left(2\phi_{y,k}^2 + 2\theta_k^2 + \epsilon_{yy}\right)\right], \tag{18}$$

where $k = 1,2$ labels the slabs. Note that the c_n are constants of order λ^0. Stability when the angular variables are all zero implies that c_1, c_2, and $2c_1 - |c_3|$ are all positive. In the undistorted phase where the angular variables are all zero one can identify the contributions of order λ of these deformations (*within the mean-field approximation*) to the elastic constants as

$$C_{11} \approx 4c_1\lambda, \quad C_{12} \approx 2c_3\lambda, \quad C_{44} \approx 4c_2\lambda. \tag{19}$$

Contributions to the elastic constants involving atomic displacements which do not distort octahedra are of order λ^0 and are not included here. As discussed in Appendix B, the mean-field estimates of Eq. (19) are unphysical because they

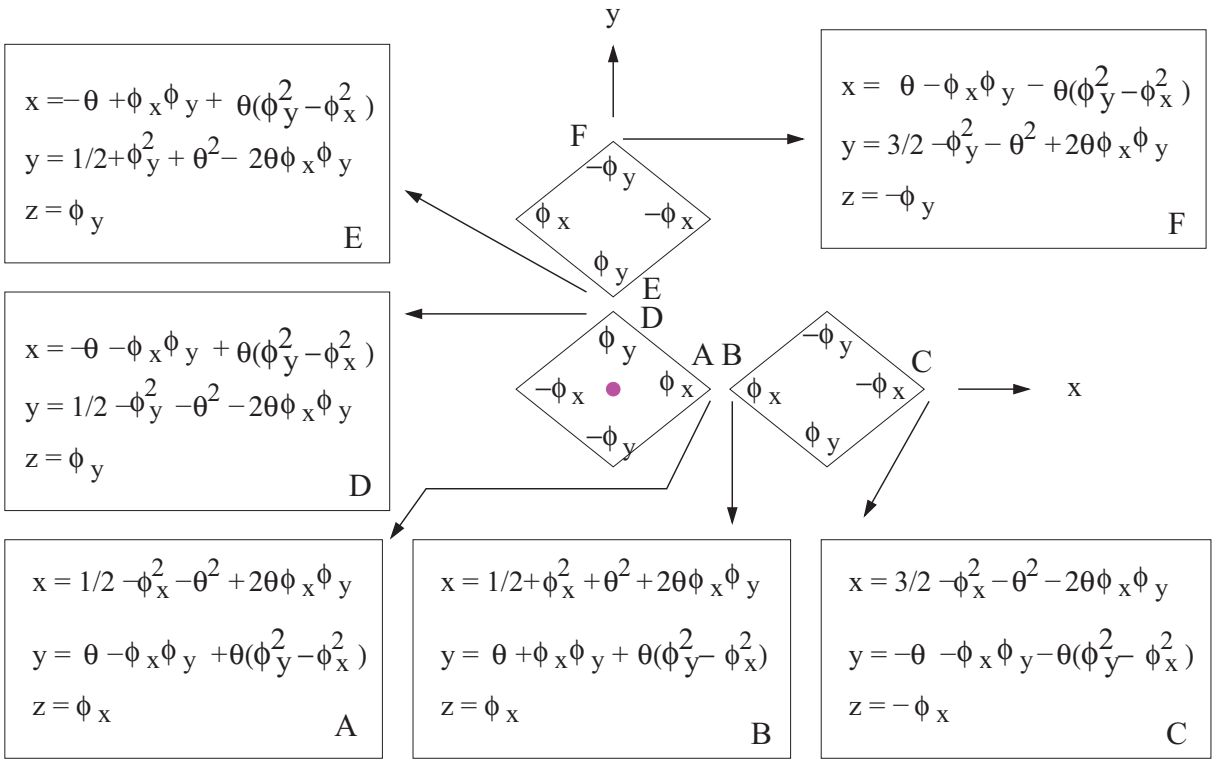

FIG. 6. (Color online) The displacements of the vertices (in the absenece of strains) for the star of **X** including nonlinear contributions up to order q^3. The origin is indicated by the (magenta) solid circle. The displacements of the octahedron at the origin are given in terms of the expansion parameters of Eq. (14). The ϕ parameters at each vertex are shown. The θ displacements are only given in the formulas. Because the wave vectors of the star of **X** are (1/2,1/2,0) and (1/2, − 1/2,0), the displacement of vertex C is related to that of vertex A by changing the signs of all the order parameters. The displacement of vertex F is obtained similarly from vertex D. The displacement of vertex B is obtained from that of vertex C by inversion about (1,0,0) and that of vertex E from that of vertex F by inversion about (0,1,0).

TABLE I. Effect of symmetry operations on the variables of the stars of $\mathbf{X} \equiv (1/2,1/2,0)$ and $\mathbf{P} \equiv (1/2,1/2,1/2)$ (shown in Fig. 5) and on the strain variables. Here $\mathcal{R}_4$ is a fourfold right-handed rotation about the positive tetragonal z axis passing through the origin, m_d and m_z are mirrors that take x into y and z into $-z$, respectively, and T is the translation $(1/2,1/2,1/2)$. The angular variables are odd under the translations $T_x = (1,0,0)$ and $T_y = (0,1,0)$. For the star of $\mathbf{X}$, $\xi = 1$ and for the star of $\mathbf{P}$, $\xi = -1$. Note that spatial inversion $\mathcal{I}$ is implicitly included because $\mathcal{I} = \mathcal{R}_4^2 m_z$ (Ref. 33). In the last line $\Omega \equiv \epsilon_{xx} - \epsilon_{yy}$.

	$\mathcal{R}_4$	m_d	m_z	T
$\phi_{x,1}$	$\phi_{y,1}$	$\phi_{y,1}$	$-\phi_{x,1}$	$\phi_{x,2}$
$\phi_{y,1}$	$-\phi_{x,1}$	$\phi_{x,1}$	$-\phi_{y,1}$	$\phi_{y,2}$
$\phi_{x,2}$	$-\phi_{y,2}$	$\phi_{y,2}$	$-\xi\phi_{x,2}$	$\xi\phi_{x,1}$
$\phi_{y,2}$	$\phi_{x,2}$	$\phi_{x,2}$	$-\xi\phi_{y,2}$	$\xi\phi_{y,1}$
θ_1	θ_1	$-\theta_1$	θ_1	θ_2
θ_2	$-\theta_2$	$-\theta_2$	$\xi\theta_2$	$\xi\theta_1$
ϵ_{xy}	$-\epsilon_{xy}$	ϵ_{xy}	ϵ_{xy}	ϵ_{xy}
Ω	$-\Omega$	$-\Omega$	Ω	Ω

do not allow for the angular variables to relieve an applied stress. However, for the purposes of analyzing the symmetry the fact that this approximation for the elastic constants does not properly allow for thermal fluctuations is not relevant.

We write the elastic free-energy density F_X for the RP214 structure of Fig. 5 for the star of $\mathbf{X}$ as

$$F_X = F_{\rm Oct} + F_2 + F_4 + F_{2\epsilon}, \tag{20}$$

where F_2 and F_4 are quadratic and quartic terms of order λ^0 and $F_{2,\epsilon}$ the order parameter strain coupling at order λ^0, which is quadratic in the order parameters and linear in the strain.

The result of Eq. (18) could be numerically verified by a first-principles calculation of the energy for the rotation of the octahedra in the two cases when (a) the lattice constants are fixed to the values appropriate to the unrotated configuration and (b) then the lattice constants are allowed to relax as the octahedra are rotated. According to Eq. (18), these two calculations should give very different results.

The free energy has to be invariant under all the symmetry operations of the "vacuum," which, in this case, is the parent tetragonal structure. Accordingly, in Table I we give the effect of symmetry operations on the variables appearing implicitly in Eq. (20). Here and below, because the octahedral constraint does not directly couple different layers, quartic terms of the form $\theta_1^2\theta_2^2$, $\phi_{x,1}^2\phi_{y,2}^2 + \phi_{x,2}^2\phi_{y,1}^2$ and $\phi_{x,1}\phi_{y,1}\phi_{x,2}\phi_{y,2}$ which are allowed by symmetry (see Table I), do not appear at order λ. (However, of course, they are present at order λ^0.) Only quartic terms which arise from the octahedral constraint at a single octahedron can appear at order λ. Using Table I, we see that the quadratic terms which are invariant under the symmetry operations which leave the reference tetragonal structure invariant are

$$\begin{aligned} F_2 &= \alpha\left[\phi_{x,1}^2 + \phi_{y,1}^2 + \phi_{x,2}^2 + \phi_{y,2}^2\right] \\ &\quad + 2\beta[\phi_{x,1}\phi_{y,2} + \phi_{x,2}\phi_{y,1}] + \gamma\left[\theta_1^2 + \theta_2^2\right] \\ &\equiv \tfrac{1}{2}[\alpha - \beta][(\phi_{x,1} - \phi_{y,2})^2 + (\phi_{x,2} - \phi_{y,1})] \\ &\quad + \tfrac{1}{2}[\alpha + \beta][(\phi_{x,1} + \phi_{y,2})^2 + (\phi_{x,2} + \phi_{y,1})] \\ &\quad + \gamma\left[\theta_1^2 + \theta_2^2\right]. \end{aligned} \tag{21}$$

Terms in $F_{2,\epsilon}$ which cause lattice distortions when tetragonal symmetry is broken are

$$\begin{aligned} F_{2,\epsilon} &= a_1\epsilon_{xy}\theta_1\theta_2 + a_2[\epsilon_{xx} - \epsilon_{yy}]\left[\phi_{x,1}^2 + \phi_{x,2}^2 - \phi_{y,1}^2 - \phi_{y,2}^2\right] \\ &\quad + a_3[\phi_{x,1}\phi_{y,1} + \phi_{x,2}\phi_{y,2}]\epsilon_{xy}. \end{aligned} \tag{22}$$

We will deal with F_4 when it is needed.

One might argue that "Constraining the form of the free energy departs ...from the accepted way of using symmetry in this theory. Any author is certainly free to postulate a modified free energy and derive consequences but the general appeal of this approach is then limited ...".[29] The reason this objection is invalid is that our treatment is predicated on the fact that these RP systems consist of rigid octahedra. (This assumption of rigidity has been accepted by the research community for several decades and is supported by recent first-principles calculations.[6,30–32]) One can imagine raising the temperature sufficiently or reducing the internal force constants so as to violate our assumption that the quartic potential due to intraoctahedral interactions dominates the quadratic terms in the Landau expansion. We refer to this limit as the limit of "octahedral melting." For the RP perovskites, this limit is clearly irrelevant in practicality. In perovskites, such as RP214, it is the geometry of the metal-oxygen bonds that leads to the rigidity of the octahedron. To ignore this physics and rely solely on symmetry (as implied by Ref. 29) is not sensible. To summarize, if it is legitimate to consider the system as consisting of rigid octahedra (as is the case for the RP perovskites), then the elastic energy quartic in the ionic displacements is dominated by coupling terms which arise from the distortion of individual octahedra. Note that the octahedra do not need to be infinitely rigid for our argument to be valid. It is only necessary that the octahedra be rigid enough that $\lambda \gg 1$; that is, that it is appropriate to consider the system as being a system of interlocking octahedra.

We now give an analysis of the above free energy which neglects fluctuations. Our plan is to eliminate the noncritical strain variables by minimizing the free energy of Eq. (20) with respect to the strains. The structural phase transitions which we are investigating arise when *one* of the channels becomes unstable, that is, when γ or $\alpha - |\beta|$ passes through zero. As in Ref. 17, we reject multicritical points where more than one channel simultaneously becomes unstable.

1. θ distortion

When only γ of Eq. (21) passes through zero, we set

$$\phi_{x,1} = \phi_{x,2} = \phi_{y,1} = \phi_{y,2} = 0. \tag{23}$$

Then, at order λ we have

$$\begin{aligned} F_{\rm Oct} &= \lambda c_1\left[\left(2\theta_1^2 + \epsilon_{xx}\right)^2 + \left(2\theta_2^2 + \epsilon_{xx}\right)^2 + \left(2\theta_1^2 + \epsilon_{yy}\right)^2\right. \\ &\quad \left.+\left(2\theta_2^2 + \epsilon_{yy}\right)^2\right] + \lambda c_3\left[\left(2\theta_1^2 + \epsilon_{xx}\right)\left(2\theta_1^2 + \epsilon_{yy}\right)\right. \\ &\quad \left.+ \left(2\theta_2^2 + \epsilon_{xx}\right)\left(2\theta_2^2 + \epsilon_{yy}\right)\right] + 2\lambda c_2\epsilon_{xy}^2. \end{aligned} \tag{24}$$

Minimizing $F_{\rm Oct}$ with respect to the strains, we get

$$\epsilon_{xx} = \epsilon_{yy} = -\left(\theta_1^2 + \theta_2^2\right) + \mathcal{O}(\lambda^{-1}). \tag{25}$$

In order to obtain ϵ_{xy} to leading order in λ we have to include the term $a_1\epsilon_{xy}\theta_1\theta_2$ from Eq. (22), so that

$$\epsilon_{xy} = -a_1\theta_1\theta_2/(4c_2\lambda) + \mathcal{O}(\lambda^{-2}). \tag{26}$$

To leading order in λ we get

$$F_{\rm Oct} = \lambda[4c_1 + 2c_3]\left[\theta_1^2 - \theta_2^2\right]^2. \qquad (27)$$

This indicates a dominant anisotropy which forces $\theta_1^2 = \theta_2^2$. It is important that this result remain true even when corrections from terms lower order in λ are included, as is discussed in Appendix A. (Otherwise, additional space groups with $\theta_1^2 \neq \theta_2^2$ would be allowed.) The result of Eq. (27) has a simple interpretation: The strain that relieves the mismatch is a uniform macroscopic strain which is only consistent with the octahedral reorientations providing they are the same in both slabs. This will be a recurring theme of our calculations.

Now we identify the space group for the above θ distortion (with $\theta_2 = \theta_1$) which is shown in panel (a) of Fig. 7. The **X** structure has generators[34] $(X \pm 1/2, Y + 1/2, Z)$, $(X, Y, Z + 1)$, $(\overline{X}, \overline{Y}, \overline{Z})$, $(X, \overline{Y}, \overline{Z})$, and $(\overline{X} + 1/2, \overline{Y}, Z + 1/2)$. In determining the space group from these generators,[35] it is useful to realize that these structures must form a subset of those listed in Ref. 17. We thus identify the space group of the structure of Fig. 7(a) as D_{2h}^{18} or $Cmca$ (64). $Cmca$ is one of the three θ-dependent structures of irrep $X_2{}^+$ for the star of **X** which are listed in Ref. 17. However, we do not allow the other two structures of Ref. 17, the first of which (D_{2h}^9 or $Pbam = 55$) has, according to Table III of Ref. 17, $|\theta_1| \neq |\theta_2|$, with $\theta_1\theta_2 \neq 0$ and the second of which (D_{4h}^5 or $P4/mbm = 127$) has, according to Table III of Ref. 17, one sublattice distorted and the other not distorted, so that $\theta_1\theta_2 = 0$ (see Fig. 7). The problem with these structures is that to avoid distorting the octahedra we had to invoke a uniform strain which only relieves the distortions in the two slabs when the distortions in the two slabs are the same. Thus, when $\theta_1^2 \neq \theta_2^2$, there is an unavoidable distortion energy of the octahedra of order λ.

Note also that both $\epsilon_{xx} = \epsilon_{yy}$ and the induced shear strain of Eq. (26) are consistent with orthorhombic axes shown in Fig. 7: The x-y shear in tetragonal coordinates is equivalent to a stretch (or compression) along the Y axis and an accompanying compression (or stretch) along the Z axis. Rotating the crystal by 90° ($\mathcal{R}_4$) changes the sign of $\theta_1\theta_2$ and thus changes the sign of ϵ_{xy}, as one would expect.

Since the octahedral constraint forces $\theta_1^2 = \theta_2^2$, we may introduce a single-order parameter $Q \equiv \theta_1$ to describe the phase transition at $T = T_0$:

$$F = \tfrac{1}{2}a(T - T_0)Q^2 + \tfrac{1}{4}uQ^4 + \tfrac{1}{6}vQ^6 + \cdots, \qquad (28)$$

where u is of order λ^0 but its sign is not fixed by symmetry. Therefore, our analysis does not imply that the ordering transition must be continuous. More generally, most of the transitions in this paper are *allowed* to be continuous, but a few must be discontinuous.

In comparison to other ordering transitions we can make an analogy between the order parameters which govern the distortion from the parent tetragonal phase and the order parameters in, say, a magnetic system. In this formulation the distortion of the parent lattice in perovskites is analogous to the development of long-range magnetic order. Having a distortion only within one sublattice of the RP system is thus analogous to having magnetic order only on some sublattices. Although one can have ordered systems which have some disordered components, they differ from the present case. For instance, the orientational phase II of solid methane (CD_4) consists of a unit cell having six orientationally ordered and two orientationally disordered molecules.[36] In that case, the site symmetry of the disordered molecules is high enough that the effective field on them from the ordered molecules vanishes.

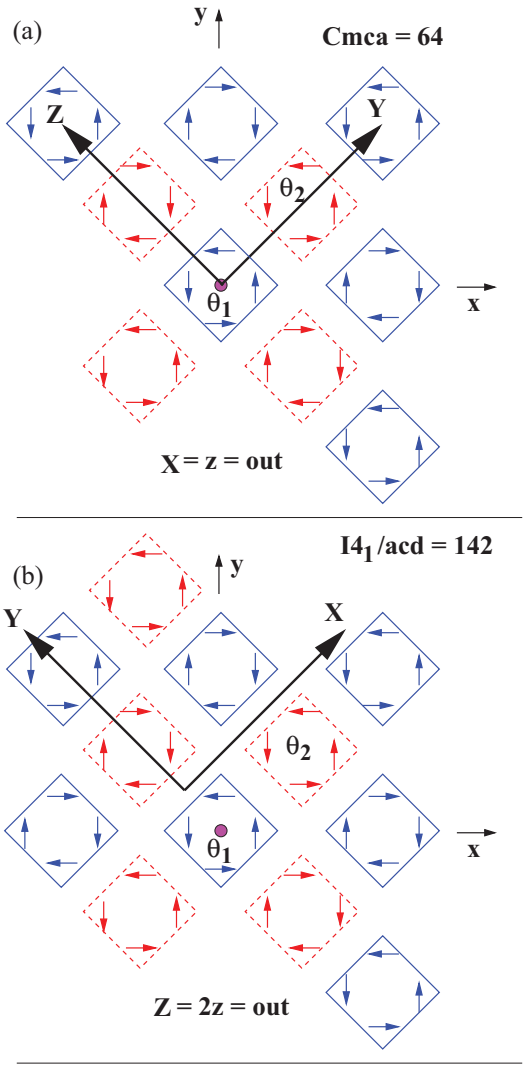

FIG. 7. (Color online) As Fig. 5. The structure of corner-sharing octahedra obtained by θ rotations for wave vector $\mathbf{X} \equiv (1/2,1/2,0)$ (top) and wave vector $\mathbf{P} \equiv (1/2,1/2,1/2)$ (bottom). The arrows indicate the displacement of the oxygens in the equatorial plane. In the top (bottom) panel the distortion is unchanged (changes sign) for $z \to z + 1$. In both panels we display structures for which $\theta_1 = \theta_2$. As noted in the text, rotating the crystal though 90° about the z axis gives a structure for which $\theta_2 = -\theta_1$. Here and in the subsequent figures we adhere to the following conventions. (1) The (magenta) solid circle indicates the original tetragonal origin, (2) the original tetragonal axes are labeled by lower case letters, (3) the axes of the distorted structure are labeled by capital letters, and (4) unless it is explicitly stated, the axes of the distorted structure which are shown are in the plane perpedicular to the original fourfold tetragonal axis. Here, in the top (bottom) panel the out-of-plane axis after distortion is $X = (0,0,1)_t$ [$Z = (0,0,2)_t$], where the subscript indicates that components are taken in the original tetragonal system. In the top (bottom) panel the distortion is unchanged (changes sign) for $z \to z + 1$. In the top (bottom) panel the new origin is at $z = 0$ ($z = 3/4$).

Furthermore, the interaction energy E between two disordered molecules is much less than kT, even at the lowest temperature at which phase II exists, so that they do not cooperatively order. Superficially, the situation here is similar to that for solid methane. For instance, suppose one builds up the distorted structure plane by plane for wave vectors in the star of **X** or **P**. The first plane would have $\theta = \theta_0$, say. Moving to the second plane we note a frustration due to the fourfold rotation, $\mathcal{R}_4$ which implies that the energy is invariant against changing the sign of θ_2. (Table I indicates that $\mathcal{R}_4$ leaves θ_1 fixed but takes θ_2 into $-\theta_2$.) If one considers the third plane, there is no analogous frustration. One will have $\theta_3 = \pm\theta_1$, the sign depending on the weak interaction between octahedra in plane 1 and those in plane 3. More generally, $\theta_{n+2} = \sigma\theta_n$, where σ can be either $+1$ or -1. If $\sigma = +1$, then $\theta_{n+2} = \theta_n$ or $\theta(z+1) = \theta(z)$ and the structure belongs to the star of **X**. If $\sigma = -1$, then $\theta_{n+2} = -\theta_n$ or $\theta(z+1) = -\theta(z)$, and the structure belongs to the star of **P**. As in quasi-two-dimensional systems, as the temperature at which the distortion becomes unstable is approached, two-dimensional correlations will become significant and then even a weak coupling in the third dimension will lead to three-dimensional long-range order at a single phase transition. This situation is reminiscent of the decoupling of magnetic sublattices in the bcc antiferromagnet.[37,38] The point is that if the distortion order parameter becomes nonzero in, say, the even-numbered planes, the mechanism that led to this order would also apply to the odd-numbered planes, which would then also distort at the same time. The distorting of both sublattices of octahedra could only be avoided if simultaneous distortions were strongly disfavored by the form of the quartic potential [i.e., if v of Eq. (4) were positive]. This possibility seems unlikely and indeed our analytic treatment of the octahedral constraint indicates that this scenario does not occur for large λ.

The free energy which includes rotation-strain coupling has a resemblance to the model of Bean and Rodbell,[39] where the spin-strain coupling in mean-field theory gives rise to a negative contribution to the term in the free energy which is quartic in the order parameter. Therefore, as the coupling is increased, mean-field theory predicts that the ordering transition changes from a continuous one to a discontinuous one. Here the situation is different. Unlike the Bean-Rodbell model, the free energy in the strong coupling limit [see Eq. (27)] does not necessarily drive the system to a first-order phase transition, at least within mean-field theory. It would be interesting to adapt the renormalization group analysis of Bergmann and Halperin[40] to elucidate the effects of orientation-strain coupling on these structural transitions.

2. ϕ distortions

Now drop the θ variables so that that the quadratic terms in the free energy, F_2 are

$$F_2 = \frac{\alpha-\beta}{2}[(\phi_{x,1}-\phi_{y,2})^2+(\phi_{x,2}-\phi_{y,1})^2] + \frac{\alpha+\beta}{2}[(\phi_{x,1}+\phi_{y,2})^2+(\phi_{x,2}+\phi_{y,1})^2]. \quad (29)$$

There are two channels of criticality, for which

$$\phi_{x,1} = \sigma\phi_{y,2}, \qquad \phi_{x,2} = \sigma\phi_{y,1}, \quad (30)$$

where $\sigma = -1$ if $\alpha-\beta$ becomes critical (zero) before $\alpha+\beta$ and $\sigma = +1$ in the reverse case.

We next consider the quartic terms of order λ. When the θ variables are dropped, $F_{\rm Oct}$ becomes

$$F_{\rm Oct} = c_1\lambda\sum_{k=1}^{2}\left[\left(2\phi_{x,k}^2+\epsilon_{xx}\right)^2+\left(2\phi_{y,k}^2+\epsilon_{yy}\right)^2\right] + c_2\lambda\sum_{k=1}^{2}[(2\phi_{x,k}\phi_{y,k}+\epsilon_{xy})^2] + c_3\lambda\sum_{k=1}^{2}\left[2\phi_{x,k}^2+\epsilon_{xx}\right]\left[2\phi_{y,k}^2+\epsilon_{yy}\right]. \quad (31)$$

Now we minimize with respect to the strains to get

$$\begin{aligned}\epsilon_{xx} &= -\left(\phi_{x,1}^2+\phi_{x,2}^2\right),\\ \epsilon_{yy} &= -\left(\phi_{y,1}^2+\phi_{y,2}^2\right),\\ \epsilon_{xy} &= -\left(\phi_{x,1}\phi_{y,1}+\phi_{x,2}\phi_{y,2}\right).\end{aligned} \quad (32)$$

Here and below we use the fact that $2c_1 - |c_3| > 0$. Thus,

$$F_{\rm Oct} = 2\lambda c_1\left[\left(\phi_{x,1}^2-\phi_{x,2}^2\right)^2+\left(\phi_{y,1}^2-\phi_{y,2}^2\right)^2\right] + 2\lambda c_3\left(\phi_{x,1}^2-\phi_{x,2}^2\right)\left(\phi_{y,1}^2-\phi_{y,2}^2\right) + 2\lambda c_2\left(\phi_{x,1}\phi_{y,1}-\phi_{x,2}\phi_{y,2}\right)^2. \quad (33)$$

Here we have a large (of order λ) anisotropy which favors having

$$\phi_{x,1} = \eta\phi_{x,2} \quad \text{and} \quad \phi_{y,1} = \eta\phi_{y,2}, \quad (34)$$

where $\eta = \pm 1$. As shown in Appendix A these conditions survive corrections from terms of lower order in λ. In particular, note that terms of order λ^0 in Eq. (22) are consistent with Eq. (32). As before, the overall sign of the quartic term is not fixed: The transition may or may not be continuous.

Now let us see what ordering vectors $\Phi \equiv [\phi_{x,1},\phi_{y,1},\phi_{x,2},\phi_{y,2}]$ are allowed by Eqs. (30) and (34). If $\alpha-\beta$ is critical, then the critical ordering vector is proportional to either $[11\bar{1}\bar{1}]$ or $[1\bar{1}1\bar{1}]$, whereas if $\alpha+\beta$ is critical, then Φ is proportional to either $[1111]$ or $1\bar{1}\bar{1}1]$. In each case, the two choices are equivalent.[41] Figure 8 shows a representative of these solutions for each case of criticality.[42]

Next, we identify the space groups of the structures of Fig. 8. The generators of $[1\bar{1}1\bar{1}]$ are $(X\pm 1/2, Y+1/2, Z)$,$(X,Y,Z+1)$, $(\overline{X},\overline{Y},\overline{Z})$, $(X,\overline{Y},\overline{Z})$, and $(\overline{X}+1/2,\overline{Y},1/2+Z)$ and those of $[\bar{1}\bar{1}11]$ (which is equivalent to $[1111]$) are $(X\pm 1/2, Y+1/2, Z)$, $(X,Y,Z+1)$, $(\overline{X},\overline{Y},\overline{Z})$, $(\overline{X},\overline{Y},Z)$, and $(X,\overline{Y},1/2+\overline{Z})$. From these generators we identify the space groups as indicated in Fig. 8. In both structures Eq. (32) gives $\epsilon_{xx} = \epsilon_{yy}$ and $\epsilon_{xy} \neq 0$. The form of these results is, of course, not modified by inclusion of corrections induced by Eq. (22) and is consistent with the orientation of the orthorhombic coordinate axes shown in Fig. 8.

Note that, in comparison to Ref. 17, our formulation does not allow the structures of space groups $Pccn$ ($D_{2h}^{10} = 56$) and $Pnnn$ ($D_{2h}^{2} = 48$). From Table III of Ref. 17 one sees that $Pccn$ has $\phi_{x,1} = \phi_{y,2} = a$ and $\phi_{y,1} = \phi_{x,2} = b$, with $a \neq b$, and $Pnnn$ has $\phi_{x,1} = -\phi_{y,2} = a$ and $\phi_{y,1} = -\phi_{x,2} = b$, with $a \neq b$. As before, to relieve the distortion of the octahedra

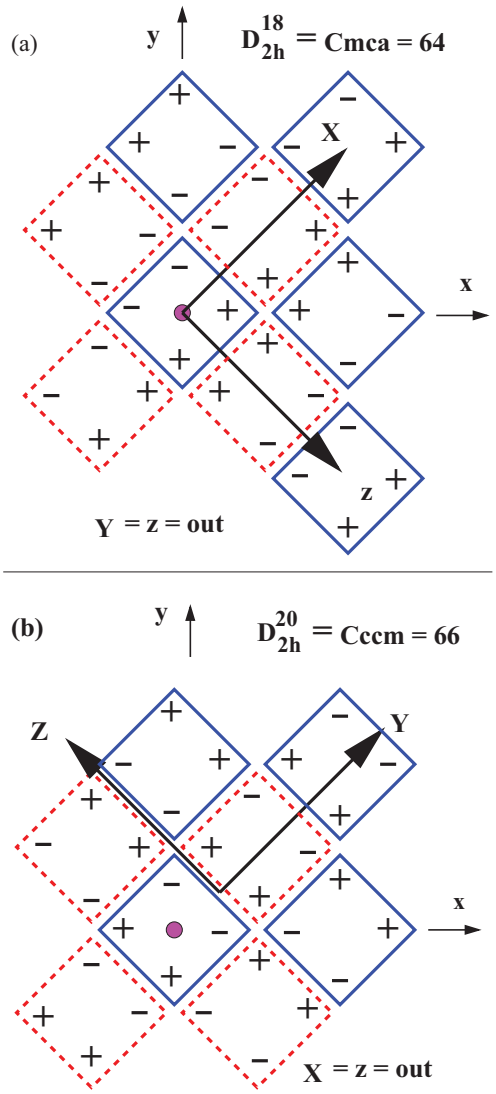

FIG. 8. (Color online) As Fig. 7 for the star of **X** (with invariance under $z \to z+1$). x, y, and z are the tetragonal axes and and X, Y, and Z are the conventional lattice vectors after distortion. The solid magenta circle is the tetragonal origin. $\Psi \equiv [\phi_{x,1},\phi_{y,1},\phi_{x,2},\phi_{y,2}] = [1\bar{1}1\bar{1}]$ for (a) and $[\bar{1}111]$ for (b) (Ref. 42). The irreps are given in Table III. The new origin has $z = 0$ for (a) and $z = 1/4$ for (b). The third new axis vector [Y for panel (a) and X for panel (b)] is $[001]_t$ in terms of the original tetragonal coordinates.

via strains implies that the order parameters have the same magnitude in both layers. Similarly we do not allow space groups $P4_2/ncm$ ($D_{4h}^{16} = 138$) and $P4_2/nnm$ ($D_{4h}^{12} = 134$) which have (in one setting) $\phi_{x,1} = \phi_{y,2} = 0$ and $|\phi_{x,2}| = |\phi_{y,1}|$. Our analysis of the space groups listed in Ref. 17 is summarized in Tables II and III.

B. The star of N

Similarly, we construct the most general structure for the star of $\mathbf{N} \equiv (1/2,0,1/2)$, whose wave vectors are $\mathbf{N}_1 \equiv (1/2,0,1/2)$, $\mathbf{N}_2 = (-1/2,0,1/2)$, $\mathbf{N}_3 = (0,1/2,1/2)$, and $\mathbf{N}_4 = (0,-1/2,1/2)$. To do this we use Fig. 9. Consider

TABLE II. Space groups of Ref. 17 for the stars if **X**, **N**, and **P** which we do not allow for RP214's. Column headings: S, stands for the Schoenflies symbol; H-M, the short Hermann-Maugin symbol as given in Ref. 8; No., the number of the space group in Ref. 8. For otherwise identical space groups, the footnotes give the basis vectors of the unit cell in terms of the original tetragonal coordinates. The irrep labels are from Ref. 17.

Irrep	S	No.	H-M	S	No.	H-M
X_2^+	D_{4h}^5	127	P_4/mbm	D_{2h}^9	55	$Pbam$
X_3^+	D_{4h}^{16}	138	$P4_2/ncm$	D_{2h}^{10}	56	$Pccn$
X_4^+	D_{4h}^{12}	134	$P4_2/nnm$	D_{2h}^2	48	$Pnnn$
N_1^+	C_{2h}^1	10	$P2/m$	C_i^1	2	$P\bar{1}$[a]
N_1^+	D_{2h}^{28}	74	$Imma$	D_{2h}^{25}	71	$Immm$
N_1^+	C_{2h}^6	15	$C2/c$	C_{2h}^3	12	$C2/m$[b]
N_1^+	C_{2h}^3	12	$C2/m$[c]	D_{4h}^{19}	141	$I4_1/amd$
N_1^+	D_{2h}^{19}	65	$Cmmm$	D_{4h}^{17}	139	$I4/mmm$
P_4	D_{4h}^{18}	140	$I4/mmm$	D_{2d}^{10}	122	$I\bar{4}2d$
P_5	D_{2h}^{28}	74	$Imma$	D_{2h}^{24}	69	$Fmmm$
P_5	S_4^2	82	$I\bar{4}$	C_{2v}^{22}	46	$Ima2$
P_5	C_{2v}^{19}	43	$Fdd2$	C_{2v}^{18}	42	$Fmm2$
P_5	D_2^9	24	$I2_12_12_1$	D_2^8	23	$I222$
P_5	C_{2h}^3	12	$C2/m$	C_2^3	5	$C2$
P_5	D_{2d}^{11}	121	$I\bar{4}2m$	D_{2d}^{12}	122	$I\bar{4}2d$
P_5	D_2^7	22	$F222$			

[a] $(\bar{1}11)$, $(1\bar{1}1)$, $(11\bar{1})$.
[b] $(00\bar{2})$, $(\bar{2}20)$, $(\bar{1}11)$.
[c] $(2,0,\bar{2})$, $(0,2,0)$, $(0,0,2)$.

first the situation in the $z = 0$ plane when we initially fix the ϕ's for octahedron A. Since the octahedra are interlocking ϕ_x has to alternate in sign as we move along x. This means that ϕ_x must be associated with a linear combination of $\mathbf{N}_1$ and $\mathbf{N}_2$ distortions. Since $N_{1,y} = N_{2,y} = 0$, we see that ϕ_x must be independent of y. Similar reasoning indicates that ϕ_y alternates along y and is therefore associated with a linear combination of $\mathbf{N}_3$ and $\mathbf{N}_4$ distortions. However, since $N_{3,x} = N_{4,x} = 0$, ϕ_y is independent of x. These wave vectors do not support nonzero values of θ. We have thereby fixed all the values of the variables in the $z = 0$ plane in terms of those of octahedron A. Now consider the situation in the $z = 1/2$ plane. Suppose we have a linear combination of $\mathbf{N}_1$ and $\mathbf{N}_2$ which gives rise to $\phi_{x,1}$ for octahedron A. If we had only $\mathbf{N}_1$, then the variables for octahedron B would be $-\phi_{x,1}$ and $-\phi_{y,1}$, whereas if we had $\mathbf{N}_2$, then these variables would be $\phi_{x,1}$ and $\phi_{y,1}$. As for the case of the star of **X**, we conclude that all the variables in the second layer are fixed in terms of the arbitrary variables of octahedron B, so that Fig. 9 characterizes the most general structure arising from the star of **N**. The effect of symmetry operations on these variables is given in Table IV.

We need to establish the analog of Fig. 6 for the star of **N**, for which, as we have already mentioned, $\theta_n = 0$. Note that for sites B and C, the sign of ϕ_y is reversed for the star of **N** in comparison to that for the star of **X**. For site A, $\mathbf{r}_A$ for the star

TABLE III. As Table II. Space groups of Ref. 17 for the stars of **X**, **N**, and **P**, which we do allow for RP214's. Under "Var." we give the variables active in the mode and under "Fig." we give the number of the illustrative figure. All phases except those of irrep $N_1{}^+$can be reached via a continuous transition.

Irrep	Var.	S	No.	H-M	Fig.
$X_2{}^+$	θ	D_{2h}^{18}	64	$Cmca$	7(a)
$X_3{}^+$	ϕ_x,ϕ_y	D_{2h}^{18}	64	$Cmca$	8(a)
$X_4{}^+$	ϕ_x,ϕ_y	D_{2h}^{20}	66	$Cccm$	8(b)
$N_1{}^+$	$\phi_x\phi_y=0$	C_{2h}^3	12	$C2/m$[a]	10(b)
$N_1{}^+$	$\phi_x^2=\phi_y^2$	C_{2h}^3	12	$C2/m$[b]	10(c)
$N_1{}^+$	$\phi_x^2\neq\phi_y^2$	C_i^1	2	$P\bar{1}$[c]	10(a)
P_4	θ	D_{4h}^{20}	142	$I4_1/acd$	7(b)
P_5[d]	ϕ_x,ϕ_y	D_{2h}^{26}	72	$Ibam$	11(a)
P_5[d]	ϕ_x,ϕ_y	C_{2h}^6	15	$C2/c$	11(c)
P_5[d]	ϕ_y	D_{2h}^{24}	70	$Fddd$	11(b)

[a]$(0\bar{1}1)$, (100), (011).
[b](002), (220), $(\frac{\bar{1}}{2}\frac{1}{2}\frac{\bar{1}}{2})$.
[c]$(\bar{1}11)$, $(\frac{1}{2}\frac{\bar{1}}{2}\frac{1}{2})$, $(11\bar{1})$.
[d]The wave vector may be close to, but not exactly at, the star of **P**.

of **N** is as in Fig. 6. However, now

$$\mathbf{r}_B=\left(1/2+\phi_x^2,-\phi_x\phi_y,\phi_x\right). \tag{35}$$

Therefore, $y_B-y_A=z_B-z_A=0$ and $x_B-x_A=2\phi_x^2$. Likewise, for site D Fig. 6 applies equally for the star of **N**. However, for sites E and F the sign of ϕ_x is reversed for the star of **N** from what it was for the star of **X**. So

$$\mathbf{r}_E=\left(-\phi_x\phi_y,1/2+\phi_y^2,\phi_y\right), \tag{36}$$

so that $x_E-x_D=z_E-z_D=0$ and $y_E-y_D=2\phi_y^2$.

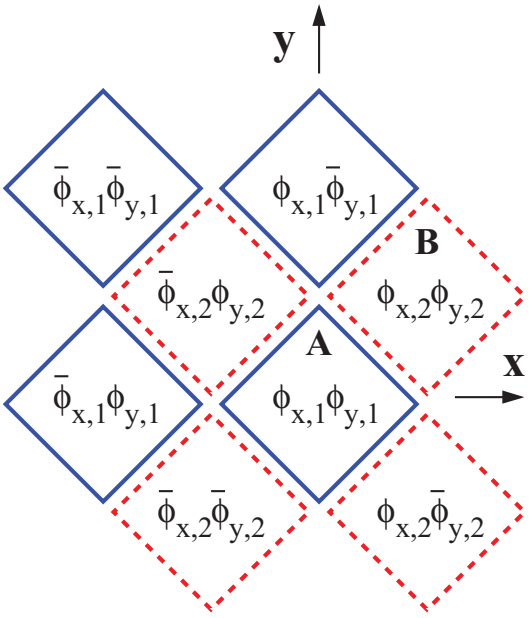

FIG. 9. (Color online) As Fig. 5. The structure of corner-sharing octahedra for the star of **N**. The variables change sign under $z\to z+1$.

TABLE IV. As Table I, but for the ϕ variables of the star of $\mathbf{N}\equiv(1/2,0,1/2)$ (shown in Fig. 9). $T\equiv(1/2,1/2,1/2)$, $T_x\equiv(1,0,0)$, and $T_y\equiv(0,1,0)$. All ϕ variables are odd under $T_z\equiv(0,0,1)$. Here $\Omega\equiv\epsilon_{xx}-\epsilon_{yy}$.

	$\mathcal{R}_4$	m_d	m_z	T	T_x	T_y
$\phi_{x,1}$	$\phi_{y,1}$	$\phi_{y,1}$	$-\phi_{x,1}$	$\phi_{x,2}$	$-\phi_{x,1}$	$\phi_{x,1}$
$\phi_{y,1}$	$-\phi_{x,1}$	$\phi_{x,1}$	$-\phi_{y,1}$	$\phi_{y,2}$	$\phi_{y,1}$	$-\phi_{y,1}$
$\phi_{x,2}$	$\phi_{y,2}$	$\phi_{y,2}$	$\phi_{x,2}$	$\phi_{x,1}$	$-\phi_{x,2}$	$\phi_{x,2}$
$\phi_{y,2}$	$\phi_{x,2}$	$\phi_{x,2}$	$\phi_{y,2}$	$\phi_{y,1}$	$\phi_{y,2}$	$-\phi_{y,2}$
ϵ_{xy}	$-\epsilon_{xy}$	ϵ_{xy}	ϵ_{xy}	ϵ_{xy}	ϵ_{xy}	ϵ_{xy}
ϵ_{xz}	ϵ_{yz}	ϵ_{yz}	$-\epsilon_{xz}$	ϵ_{xz}	ϵ_{xz}	ϵ_{xz}
ϵ_{yz}	$-\epsilon_{xz}$	ϵ_{xz}	$-\epsilon_{yz}$	ϵ_{yz}	ϵ_{yz}	ϵ_{yz}
Ω	$-\Omega$	$-\Omega$	Ω	Ω	Ω	Ω

We now write the Landau expansion for the star of **N**. Taking account of the symmetries of Table IV and the preceding discussion, we obtain the octahedral distortion energy for the star of **N** to be

$$F_{\rm Oct}=c_1\lambda\sum_{k=1}^{2}\left[\left(2\phi_{x,k}^2+\epsilon_{xx}\right)^2+\left(2\phi_{y,k}^2+\epsilon_{yy}\right)^2\right]+c_3\lambda\sum_{k=1}^{2}\left(2\phi_{x,k}^2+\epsilon_{xx}\right)\left(2\phi_{y,k}^2+\epsilon_{yy}\right). \tag{37}$$

When $F_{\rm Oct}$ is minimized with respect to the strains we find that

$$\begin{aligned}\epsilon_{xx}&=-\left(\phi_{x,1}^2+\phi_{x,2}^2\right),\\ \epsilon_{yy}&=-\left(\phi_{y,1}^2+\phi_{y,2}^2\right),\end{aligned} \tag{38}$$

which leads to the result that

$$F_{\rm Oct}=2c_1\lambda\left[\left(\phi_{x,1}^2-\phi_{x,2}^2\right)^2+\left(\phi_{y,1}^2-\phi_{y,2}^2\right)^2\right]+2c_3\lambda\left[\left(\phi_{x,1}^2-\phi_{x,2}^2\right)\left(\phi_{y,1}^2-\phi_{y,2}^2\right)\right]. \tag{39}$$

At order λ this anisotropy favors having

$$\phi_{x,1}=\sigma\phi_{x,2},\quad \phi_{y,1}=\eta\phi_{y,2}, \tag{40}$$

with $\sigma=\pm1$ and $\eta=\pm1$. As discussed in Appendix A, this result is stable against inclusion of terms of lower order in λ.

Now the free energy is

$$F=F_{\rm Oct}+F_4+F_2+F_\epsilon, \tag{41}$$

where F_4 consists of the quartic terms of order λ^0:

$$F_4=\frac{u}{4}\left[\left(\phi_{x,1}^2+\phi_{y,1}^2\right)^2+\left(\phi_{x,2}^2+\phi_{y,2}^2\right)^2\right]+v\left(\phi_{x,1}^2\phi_{y,1}^2+\phi_{x,2}^2\phi_{y,2}^2\right)+w\left(\phi_{x,1}^2\phi_{x,2}^2+\phi_{y,1}^2\phi_{y,2}^2\right)+x\left(\phi_{x,1}^2\phi_{y,2}^2+\phi_{y,1}^2\phi_{x,2}^2\right). \tag{42}$$

F_2 consists of the quadratic terms of order λ^0:

$$F_2=\alpha\left[\phi_{x,1}^2+\phi_{y,1}^2+\phi_{x,2}^2+\phi_{y,2}^2\right], \tag{43}$$

and the interaction F_ϵ between strains and octahedral rotations is

$$F_\epsilon=b_1[\epsilon_{xz}\phi_{x,1}\phi_{x,2}+\epsilon_{yz}\phi_{y,1}\phi_{y,2}]+b_2[\epsilon_{xx}-\epsilon_{yy}]\left[\phi_{x,1}^2-\phi_{y,1}^2+\phi_{x,2}^2-\phi_{y,2}^2\right]+b_3\epsilon_{xy}\phi_{x,1}\phi_{y,1}\phi_{x,2}\phi_{y,2}+\cdots, \tag{44}$$

where the dots indicate terms which do not break tetragonal symmetry. We used the results of Table IV to ensure that the above free energy consisted of terms invariant under the symmetry of the vacuum.

We are studying the transition which occurs when α of Eq. (43) passes through zero. The possible directions in the four-dimensional space of these critical variables in which ordering actually occurs is dictated by the form of F_4, whose effect we now study. When Eq. (40) is satisfied, F_4 becomes

$$F_4 = 2(v - w + x)\phi_x^2\phi_y^2 + [w + (u/2)]\left(\phi_x^2 + \phi_y^2\right)^2, \quad (45)$$

where $\phi_x^2 = \phi_{x,1}^2 = \phi_{x,2}^2$ and $\phi_y^2 = \phi_{y,1}^2 = \phi_{y,2}^2$. This indicates that we can have a structural phase transition into three classes of states. We can have a continuous phase transition into states of class A with $\phi_x^2 = \phi_y^2$ if $(v - w + x)$ is negative or into a state of class B with $\phi_x\phi_y = 0$ if $(v - w + x)$ is positive. In addition, we can have a phase transition to a state of class C in which ϕ_x and ϕ_y do not assume special values if the higher-order terms cause the transition to be discontinuous. The next step is to determine which of these solutions are inequivalent, that is, which are not related by a symmetry operation.[41]

We first show that all solutions of class A are equivalent to one another. Using the results given in Table IV we have that

$$\left(1 + \mathcal{R}_4 + \mathcal{R}_4^2 + \mathcal{R}_4^3\right)[1111] = [\{\mu\nu\}11], \quad (46)$$

where $\{\mu\nu\}$ indicates the set of μ, ν values, that is, $\{\mu\nu\} = 11 + 1\bar{1} + \bar{1}1 + \bar{1}\bar{1}$. Then

$$T\left(1 + \mathcal{R}_4 + \mathcal{R}_4^2 + \mathcal{R}_4^3\right)[1111] = [11\{\mu\nu\}] \equiv \Phi, \quad (47)$$

and finally

$$\left(1 + \mathcal{R}_4 + \mathcal{R}_4^2 + \mathcal{R}_4^3\right)\Phi = [\{\rho\tau\}\{\mu\nu\}], \quad (48)$$

where (apart from an arbitrary overall amplitude) the right-hand side of this equation includes all vectors of class A. In class A, $\phi_x^2 = \phi_y^2$, and we take $[\bar{1}1\bar{1}\bar{1}]$ as its representative.

Next we consider solutions of class B. From Table IV note that

$$\left[1 + \mathcal{R}_4^2\right][1 + T_x][1010] = \sum_{\mu\nu=\pm1}[\mu 0\nu 0] \equiv \Phi \quad (49)$$

and

$$\mathcal{R}_4\Phi = \sum_{\mu\nu=\pm1}([\mu 0\nu 0] + [0\mu 0\nu]). \quad (50)$$

The right-hand side includes all vectors of class B. We may take $[010\bar{1}]$ as the representative of class B.

Finally, we consider solutions of class C, which are of the form $[x, y, \pm x, \pm y]$, where $|x| \neq |y|$ and both are nonzero. Using Table IV we write

$$m_d\mathcal{R}_4[xyxy] = [x\bar{y}xy] \quad (51)$$

so that

$$[1+m_z][1+m_d\mathcal{R}_4][x,y,x,y] = \sum_{\sigma_1,\sigma_2=\pm1}[\sigma_1 x,\sigma_2 y,x,y]. \quad (52)$$

From this we conclude that all vectors of class C are equivalent to one another, and we take their representative to be $[\bar{x}y\bar{x}y]$.

Thus, in all, we have the three allowed space groups from the star of **N** shown in Fig. 10: $[\bar{x}y\bar{x}y]$, $[010\bar{1}]$, and $[\bar{1}\bar{1}\bar{1}\bar{1}]$. As before, to determine the space groups of the structures we use Fig. 10 to write down their generators.

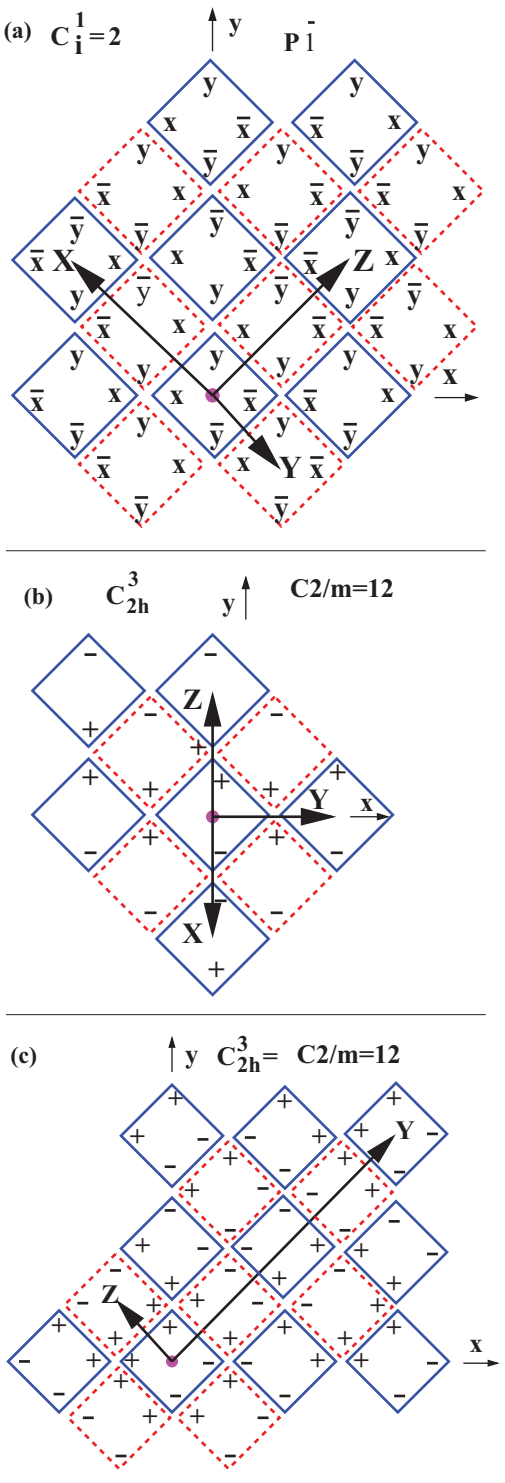

FIG. 10. (Color online) As Fig. 8 for the star of **N** (with sign change under $z \to z + 1$) for (a) (class C) $[\bar{x}y\bar{x}y]$, (b) (class B) $[010\bar{1}]$, and (c) (class A) $[\bar{1}\bar{1}\bar{1}\bar{1}]$. x, y, and z are the tetragonal axes, and X, Y, and Z are $[(\bar{1}11),(1/2,-1/2,1/2),(11\bar{1})]$ in (a), $[(0\bar{1}1),(100),(011)]$ in (b), and $[(002),(220)(-1/2,1/2,-1/2)]$ in (c). All the new origins are at $z = 0$.

For $[\bar{x}y\bar{x}y]$ the generators are $(X+1,Y,Z)$, $(X,Y+1,Z)$, $(X,Y,Z+1)$, and $(\bar{X},\bar{Y},\bar{Z})$, which is C_i^1 $(P\bar{1} = 2)$. For both $[010\bar{1}]$ and $[\bar{1}\bar{1}\bar{1}\bar{1}]$, the generators are $(X,Y,Z+1)$, $(X+1/2,Y+1/2,Z)$, $(X+1/2,Y-1/2,Z)$, $(\bar{X},\bar{Y},\bar{Z})$, and

$(\overline{X},Y,\overline{Z})$, which is C_{2h}^3 ($C2/m = 12$). Although these two structures belong to the same space group, they are different because their unit cells are different (see Fig. 10).

Finally, we discuss the strains which are induced by the lowering of symmetry from the tetragonal parent structure. First consider the structures of class A which have $\phi_{x,1}^2 = \phi_{y,1}^2 = \phi_{x,2}^2 = \phi_{y,2}^2$. A representative of this family is shown in Fig. 10(c). Note that in space group $C2/m$ the Y axis is an axis of twofold rotation symmetry and is perpendicular to the X-Z pane, but X and Z make an arbitrary angle with one another. Therefore, we expect that ϵ_{xx} must be equal to ϵ_{yy} as predicted by Eq. (38). Also we expect, in agreement with Eq. (44), that ϵ_{xy} is nonzero since the tetragonal [110] and [1$\overline{1}$0] directions are not symmetry related in the distorted phase. Also, since X need no longer be perpendicular to the x-y plane, ϵ_{xz} and ϵ_{yz} should not vanish. This is exactly what Eq. (44) predicts. The term proportional to b_1 in Eq. (44) implies that for the representative shown in Fig. 10(c) $\epsilon_{xz} = -\epsilon_{yz}$, so that the X axis is tipped *in the plane perpendicular to* Y. The angle between X and Z is not fixed by symmetry but Y must be perpendicular to both X and Z. The strains for states of class B [see Fig. 10(b)] with $\Psi = [\mu 0 \nu 0]$ or $[0\mu 0\nu]$ with $\mu^2 = \nu^2$ are discussed similarly. Here to have Y be perpendicular to X and Z we must have $\epsilon_{xy} = 0$, but $\epsilon_{xx} - \epsilon_{yy}$ is nonzero. Also the term in b_1 in Eq. (44) is such that the z axis is tipped in the plane perpendicular to Y (which for this representative coincides with x). All these observations are again consistent with Eq. (44). The strains for class C, a representative of which is shown in Fig. 10(a), are unconstrained since the distorted structure has only inversion symmetry.

In Table III (II) we list the structures which are (not) allowed. We only allow one of the eight structures for the irrep ${N_1}^+$ listed in Ref. 17 which occur via a discontinuous transition. In addition, Ref. 17 lists two space groups $Cmmm$ (65) for which $\Psi = [1000]$ and $I4/mmm$ (139) for which $\Psi = [1100]$. Since these structures have undistorted sublattices, they are inconsistent with the rigid octahedral constraint because the octahedral distortion cannot be relieved by a uniform strain. They are also counterintuitive in that they both describe states in which nonzero order parameters appear only on alternate planes. (Look back at the discussion in Sec. III A 1, "In comparison to other ordering transitions . . .".)

C. The star of P

The star of **P** consists of the vectors $\mathbf{P}_1 \equiv (1/2,1/2,1/2)$ and $\mathbf{P}_2 \equiv (1/2,-1/2,1/2)$. The possible structures are identical to those for the star of **X**, except that the variables change sign under $z \to z+1$ as indicated in Fig. 5. The transformation properties of these variables are given in Table I. The quartic terms are the same as for the star of **X**. However, the quadratic terms differ because of the ξ factors that appear in Table I. The octahedral constraint assumes the same form as for the star of **X** because the stars of **X** and **P** differ only in how the layers are stacked.

1. θ distortions

We analyze these as before. In the channel where γ of Eq. (21) passes through zero, since the octahedral constraint is the same as for the star of **X**, we again have (for this channel) Eq. (27):

$$F_{\rm Oct} = \lambda[4c_1 + 2c_3]\left[\theta_1^2 - \theta_2^2\right]^2, \tag{53}$$

so that $|\theta_1| = |\theta_2|$. This structure has the same degeneracy associated with the relative phase of even and odd layers that we saw for the previous θ structures (at the star of **X**). Because $P_z = 1/2$, the only θ-dependent structure has $\theta_{n+2} = -\theta_n$. The other two structures listed in Ref. 17 which have $|\theta_1| \neq |\theta_2|$ are not admissible because the octahedral distortion cannot be removed by a uniform strain if $|\theta_1| \neq |\theta_2|$. The allowed **P** structure, shown in Fig. 7(b) has generators $(X - 1/2, Y + 1/2, Z + 1/2)$, $(X + 1/2, Y - 1/2, Z + 1/2)$, $(X + 1/2, Y + 1/2, Z - 1/2)$, $(\overline{X},\overline{Y},\overline{Z})$, $(X,\overline{Y},\overline{Z} + 1/2)$, and $(\overline{Y} + 1/4, X + 3/4, Z + 1/4)$, which is space group D_{4h}^{20} or $I4_1/acd$ (142).

2. ϕ distortions

Now consider the ϕ-dependent solutions which are associated with irrep P_5 according to Ref. 17. Note that all the subgroups from this irrep listed there and in Ref. 19 do not satisfy the Lifshitz condition. What this means is that the quadratic instability occurs at a wave vector that is not fixed by symmetry[43] (so that it cannot be assumed to be at the star of **P**). Accordingly, the wave vector can only be at the star of **P** if the transition is discontinuous.

However, we can determine which structures with wave vectors either at or near the star of **P** can be condensed. To do this, we simply ignore the Lifshitz criterion in our analysis of the free energy. As for the θ structures, the octahedral distortion energy is the same as for the star of **X** and is therefore given by Eq. (33). Thus, as before,

$$\phi_{x,1} = \eta\phi_{x,2} \quad \text{and} \quad \phi_{y,1} = \eta\phi_{y,2}, \tag{54}$$

where $\eta = \pm 1$. From Table I one sees that $m_z\eta = -\eta$, so that we only need consider the case $\eta = 1$. The quadratic terms are different than those of the star of **X** because of the appearance of the ξ factors in Table I. Thus, the quadratic terms are

$$F_2 = \alpha\left[\phi_{x,1}^2 + \phi_{y,1}^2 + \phi_{x,2}^2 + \phi_{y,2}^2\right]. \tag{55}$$

As before, we identify the space groups of these solutions by determining the generators of the inequivalent representatives shown in Fig. 11. For (a) ($[\overline{1}1\overline{1}1]$) the generators are[44] $(X,Y,\overline{Z})$, $(X,\overline{Y},\overline{Z} + 1/2)$, $(\overline{X},\overline{Y},\overline{Z})$, $(X - 1/2, Y + 1/2, Z + 1/2)$, $(X + 1/2, Y - 1/2, Z + 1/2)$, $(X + 1/2, Y + 1/2, Z - 1/2)$ and thus the space group is $Ibam$ ($D_{2h}^{26} = 72$). For (b) ($[0\overline{1}0\overline{1}]$) the generators are $(\overline{X} + 1/4, \overline{Y} + 1/4, Z)$, $(X,\overline{Y} + 1/4,\overline{Z} + 1/4)$, $(\overline{X},\overline{Y},\overline{Z})$, $(X, Y + 1/2, Z + 1/2)$, $(X + 1/2, Y, Z + 1/2)$, $(X + 1/2, Y + 1/2, Z)$, and thus the space group is $Fddd$ ($D_{2h}^{24} = 70$). For (c) ($[xyxy]$) the generators are $(\overline{X}, Y, \overline{Z} + \frac{1}{2})$, $(\overline{X},\overline{Y},\overline{Z})$, $(X + 1/2, Y + 1/2, Z)$, $(X - 1/2, Y + 1/2, Z)$, $(X, Y, Z + 1)$ and thus the space group is $C2/c$ ($C_{2h}^6 = 15$). When the Lifshitz instability is resolved, these space groups give rise either to commensurate structures at the star of **P** via a first-order transition or to structures having incommensurate wave vectors near the star of **P**. If the wave vector is not exactly at **P**, then the lattice distortion has to also be incommensurate.

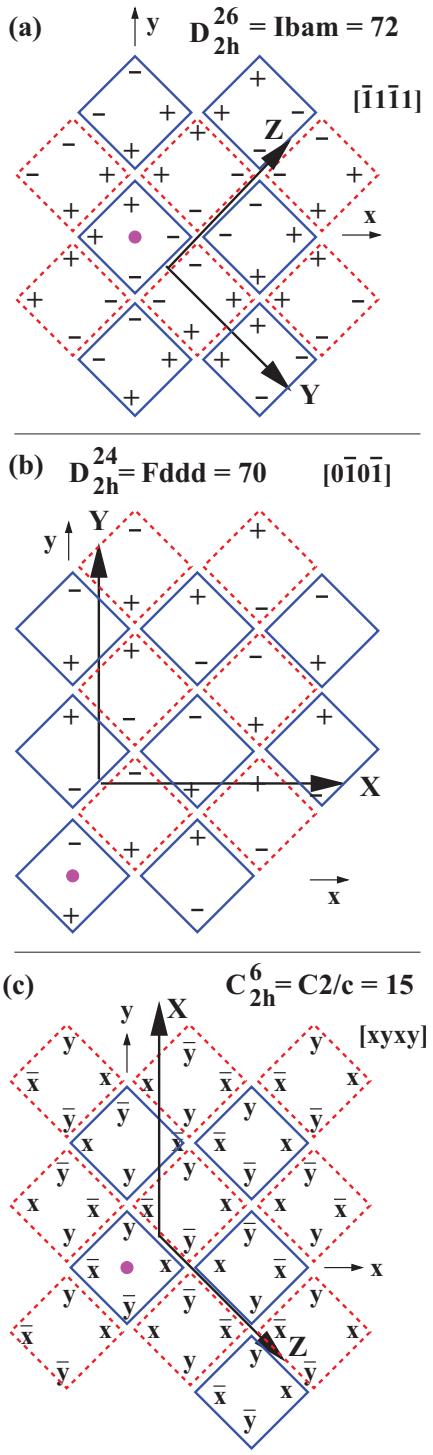

FIG. 11. (Color online) As Fig. 8 for the star of **P** (variables change sign under $z \to z+1$). x, y, and z are the tetragonal axes and and X, Y, and Z are axes of the distorted structure. The new origins are in the $z = 3/4$ plane except for (c), where $z = 1/4$. The new out-of-plane lattice vector, X for (a), Z for (b), and Y for (c), has magnitude 2 and is along z. The actual structures may involve an incommensurate wave vector near the star of **P**.

IV. RP327 STRUCTURES

In this section we perform the same analysis for the $n = 2$ RP systems $A_3B_2C_7$, which we call the RP327 systems. As shown in Fig. 1, these systems consist of two slabs. Each slab consists of two layers which we label a and b (or 1 and 2). If we fix the ϕ variables in layer a, the octahedral constraint fixes each ϕ variable in layer b to be the negative of its nearest neighbor in layer a. As a result, each structure of the RP327 system is characterized by the same number of ϕ variables as its analog for the RP214 system. In contrast, since there is no such relation between the θ variables of layers a and b, we introduce variables $\theta_{k\alpha}$ to describe the rotation within the αth layer ($\alpha = a,b$) of the kth slab ($k = 1,2$), as shown in Fig. 12. The transformation properties of the variables are summarized in Table V.

TABLE V. As Table I for the stars of **X** and **P**, except that this table is for the variables of RP327 systems. The first and second indices on θ label the slab and layer, respectively. The first and second indices on ϕ label the component and slab, respectively. Note that $z = 0$ (about which m_z is taken) is midway between layers a and b. T is the translation $(1/2,1/2,1/2)$.

	$\mathcal{R}_4$	m_d	m_z	T
$\theta_{1,a}$	$\theta_{1,a}$	$-\theta_{1,a}$	$\theta_{1,b}$	$\theta_{2,a}$
$\theta_{1,b}$	$\theta_{1,b}$	$-\theta_{1,b}$	$\theta_{1,a}$	$\theta_{2,b}$
$\theta_{2,a}$	$-\theta_{2,a}$	$-\theta_{2,a}$	$\xi\theta_{2,b}$	$\xi\theta_{1,a}$
$\theta_{2,b}$	$-\theta_{2,b}$	$-\theta_{2,b}$	$\xi\theta_{2,a}$	$\xi\theta_{1,b}$
$\phi_{x,1}$	$\phi_{y,1}$	$\phi_{y,1}$	$\phi_{x,1}$	$\phi_{x,2}$
$\phi_{y,1}$	$-\phi_{x,1}$	$\phi_{x,1}$	$\phi_{y,1}$	$\phi_{y,2}$
$\phi_{x,2}$	$-\phi_{y,2}$	$\phi_{y,2}$	$\xi\phi_{x,2}$	$\xi\phi_{x,1}$
$\phi_{y,2}$	$\phi_{x,2}$	$\phi_{x,2}$	$\xi\phi_{y,2}$	$\xi\phi_{y,1}$

A. The star of X

1. θ structures

The distortion energy at order λ in the notation of Eq. (18) is (when, as before, $\epsilon_{xy} = 0$)

$$F_{\rm Oct} = c_1\lambda \sum_{k,\alpha}\left[\left(2\theta_{k,\alpha}^2 + \epsilon_{xx}\right)^2 + \left(2\theta_{k,\alpha}^2 + \epsilon_{yy}\right)^2\right] + c_3\lambda \sum_{k,\alpha}\left[\left(2\theta_{k,\alpha}^2 + \epsilon_{xx}\right)\left(2\theta_{k,\alpha}^2 + \epsilon_{yy}\right)\right], \quad (56)$$

where the sums are over $k = 1,2$ and $\alpha = a,b$. When $F_{\rm Oct}$ is minimized with respect to the strains, one finds that

$$\epsilon_{xx} = \epsilon_{yy} = -\frac{1}{2}\sum_{k,\alpha}\theta_{k,\alpha}^2 \quad (57)$$

and

$$F_{\rm Oct} = 4\lambda[2c_1 + c_3]\left[\sum_{k,\alpha}\theta_{k,\alpha}^4 - \frac{1}{4}\left(\sum_{k,\alpha}\theta_{k,\alpha}^2\right)^2\right]. \quad (58)$$

Using the symmetry operations of Table V we find that the free energy of the θ structures for the star of **X** assumes the form

$$F(\theta) = 4\lambda[2c_1 + c_3]\left[\sum_{k,\alpha}\theta_{k,\alpha}^4 - \frac{1}{4}\left(\sum_{k,\alpha}\theta_{k,\alpha}^2\right)^2\right] + \sum_{k=1}^{2}\left[\frac{a}{2}\left(\theta_{ka}^2 + \theta_{kb}^2\right) + b\theta_{ka}\theta_{kb}\right] + F_4, \quad (59)$$

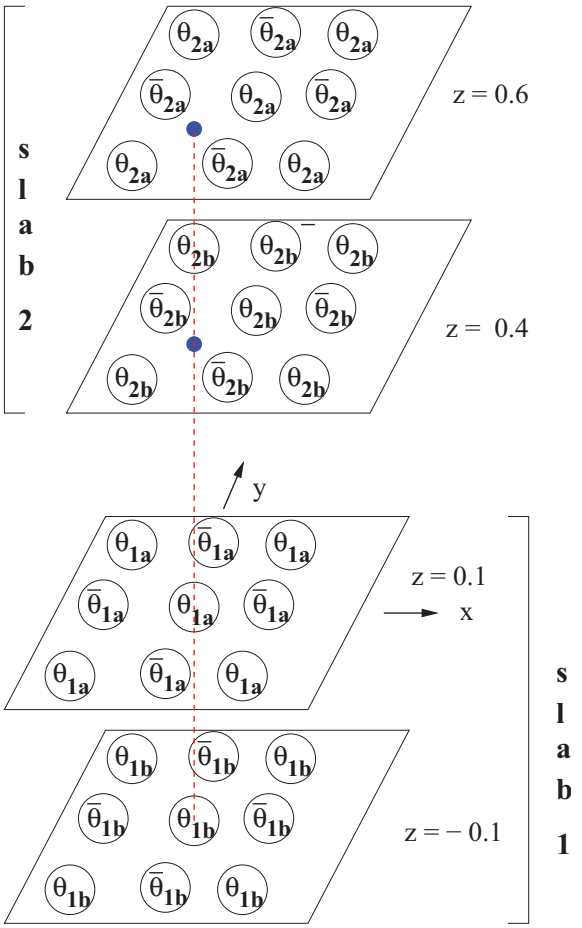

FIG. 12. (Color online) Values of the rotation (θ) variables in different z-planes for the most general such distortion of RP327's for the stars of **X** and **P**. The (red) dashed line is the axis about which the fourfold rotation $\mathcal{R}_4$ is taken and the (blue) dots show the points $x = y = 0$ in the $z = 0.4$ and $z = 0.6$ planes. Under $\mathcal{R}_4$ an octahedron in slab 1 is taken either into itself or into an equivalent octahedron. Under $\mathcal{R}_4$ an octahedron in slab 2 is taken into another whose rotation angle is of opposite sign. For the star of **X**, $\theta(z+1) = \theta(z)$ and for the star of **P**, $\theta(z+1) = -\theta(z)$.

where F_4 denotes the quartic terms of order λ^0. For large λ, the minima of this free energy at criticality when $(a - |b|)$ passes through zero occur for

$$\theta_{1a} = -\frac{b}{|b|}\theta_{1b}, \quad \theta_{2a} = -\frac{b}{|b|}\theta_{2b}, \quad \theta_{2,a}^2 = \theta_{1,a}^2. \tag{60}$$

Thus, as shown in Fig. 13, we have two possible distorted structures, depending on the sign of b:

$$\theta_{1,a} = -\theta_{1,b} = \xi\theta_{2,a} = -\xi\theta_{2,b}, \quad b > 0, \tag{61}$$

$$\theta_{1,a} = \theta_{1,b} = \xi\theta_{2,a} = \xi\theta_{2,b}, \quad b < 0, \tag{62}$$

where $\xi = \pm 1$. The fact that ξ can have either sign indicates the decoupling of even and odd numbered sublattices which we mentioned in connection with the analogous RP214 θ structures.

We now determine the space groups corresponding to these two modes. In the mode of Eq. (62) the two layers can be coalesced continuously into a single layer. So this RP327

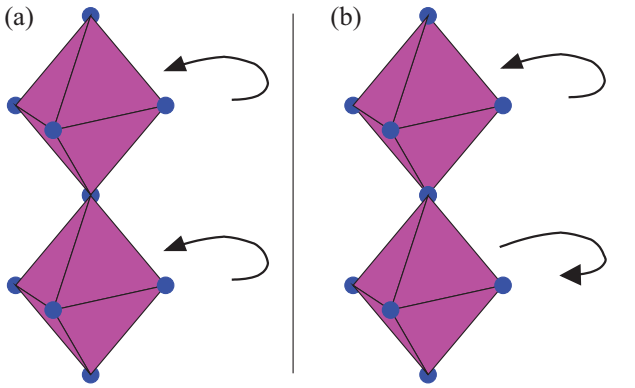

FIG. 13. (Color online) The two θ modes for a bilayer. (Left) The two layers rotate in phase as in Eq. (62). (Right) The two layers rotate out of phase as in Eq. (61). The out-of-phase rotation increases the energy by twisting the oxygen orbitals but this is compensated by reducing the Coulomb interactions between octahedra. First-principles calculations (Ref. 32) indicate that these modes differ only slightly in energy.

structure has the same symmetry as the $Cmca$ θ structure for RP214 resulting from the star of **X**. The RP327 structure is obtained by replacing the single layer slab of the RP214 structure by a two-layer slab in which the two layers are rotated in phase as in Fig. 13(a). The mode of Eq. (61) is shown in Fig. 14(a). We have to discuss the way we depict bilayer systems in our figures. Within each square (which represents the equatorial oxygens of an octahedron) the symbols closer to the corners of the square apply to the upper layer of the bilayer and the symbols closer to the center apply to the lower layer of the bilayer. This convention is convenient for visualizing the effect of rotations about an axis perpendicular to the plane of the paper. However, note that operations such as reflection through the plane of the paper or inversion relative to the center of the octahedron lead to an interchange of inner and outer symbols. Experience indicates that for these operations one should use the results of Fig. 15, supplemented, if need be, by a translation. Operations such as $\mathcal{O} = (x,\overline{y},\overline{z})$ which involve taking z into $-z$ are best expressed as $\mathcal{O} = \mathcal{I}(\overline{x},y,z)$ or $\mathcal{O} = m_z(x,\overline{y},z)$. The mirror planes perpendicular to the page do not cause any confusion because for them outer symbols are taken into outer symbols, thus avoiding visual complications. We now return to the discussion of the mode of Eq. (61) in Fig. 14(a). Using, if need be, the results of Fig. 15, one sees that this structure has generators $(X \pm 1/2, Y + 1/2, Z)$, $(X, Y, Z + 1)$, $(\overline{X}, \overline{Y}, \overline{Z})$, $(X + 1/2, \overline{Y}, \overline{Z} + 1/2)$, and $(\overline{X} + 1/2, \overline{Y}, Z)$, which therefore is $Ccca$ (D_{2h}^{22}) 68 coming from irrep $X_1{}^-$.

2. ϕ structures

Now we analyze the free energy for ϕ distortions at the star of **X**. Since ϕ_x and ϕ_y alternate in sign from one layer to the next in each slab, we characterize the structures by the values of ϕ_x (ϕ_y) in the *top* layer of the kth slab, which we denote $\phi_{x,k}$ ($\phi_{y,k}$). Here the effect of m_z has the opposite sign from the RP214 case. However, since all terms are of even order in the ϕ's, the symmetry of the free energy is the same as for

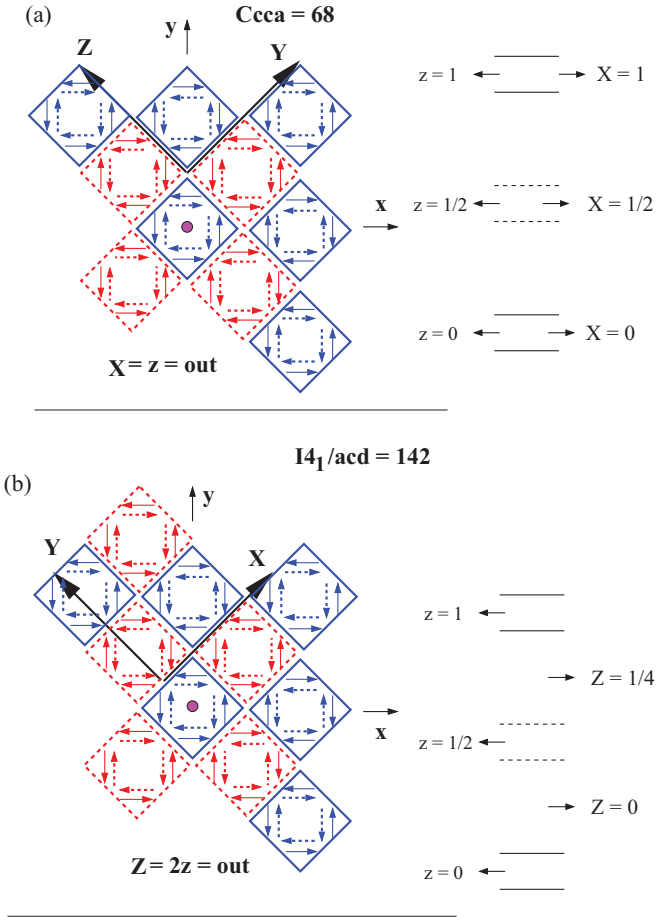

FIG. 14. (Color online) As Fig. 7. The θ modes with $\theta_{n,a} = -\theta_{n,b}$. The full (dashed) squares are equatorial sections of the bilayer centered at $z = 0$ ($z = 1/2$). The outer full (inner dashed) arrows are the displacements of the equatorial oxygens in the equatorial plane in the upper (lower) layer of the bilayer. The upper (lower) panel is associated with the star of **X** (**P**). In the upper (lower) panel the arrows are unchanged (reversed) under $z \to z + 1$. For panel a (b) the X (Z) axis for the distorted structure is $[0,0,1]_t$ ($[0,0,2]_t$) and the new origin is at $z = 0$ (at $z = 1/4$). At right we show the tetragonal z coordinates (and the distorted X or Z coordinates) of the full and dashed layers.

RP214. So

$$
\begin{aligned}
F = {} & 4c_1\lambda\left[\left(\phi_{x,1}^2 - \phi_{x,2}^2\right)^2 + \left(\phi_{y,1}^2 - \phi_{y,2}^2\right)^2\right] \\
& + 4c_3\lambda\left(\phi_{x,1}^2 - \phi_{x,2}^2\right)\left(\phi_{y,1}^2 - \phi_{y,2}^2\right) \\
& + [(\alpha - \beta)/2][(\phi_{x,1} - \phi_{y,2})^2 + (\phi_{x,2} - \phi_{y,1})^2] \\
& + [(\alpha + \beta)/2][(\phi_{x,1} + \phi_{y,2})^2 + (\phi_{x,2} + \phi_{y,1})^2]. \qquad (63)
\end{aligned}
$$

The analysis parallels that for RP214 systems. From the first two lines we conclude that $\phi_{x1}^2 = \phi_{x2}^2$ and $\phi_{y1}^2 = \phi_{y2}^2$. There are two cases. The first is if $\alpha - \beta$ is critical so that $\phi_{x1} = -\phi_{y2}$ and $\phi_{x2} = -\phi_{y1}$. The second is if $\alpha + \beta$ so that $\phi_{x2} = \phi_{y1}$ and $\phi_{x1} = \phi_{y2}$. For the first case the possible ordering vectors are proportional to $\Phi = [11\bar{1}\bar{1}]$ or $[1\bar{1}1\bar{1}]$. These are equivalent structures and we take the second one as the representative for this case. For the second case the possible ordering vectors are proportional to $\Phi = [1111]$ and $[1\bar{1}\bar{1}1]$. These are equivalent structures and we take $[\bar{1}\bar{1}\bar{1}\bar{1}]$ as the representative for this case. Figure 16 shows these representatives.

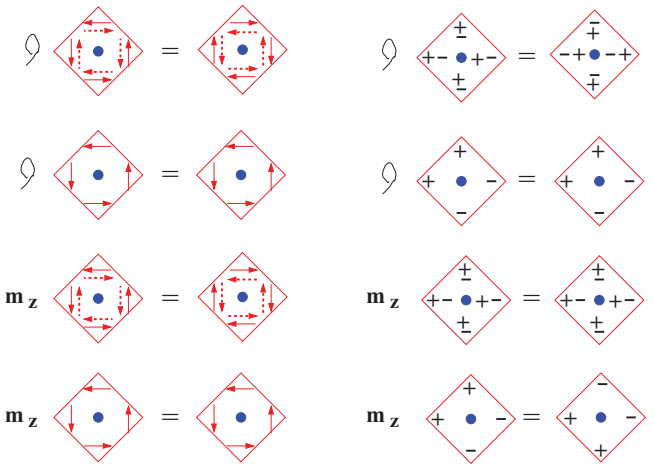

FIG. 15. (Color online) The effect of the operations (a) inversion and and (b) m_z which take z into $-z$. Here the distortion of a bilayer is represented by two sets of symbols within the square representing the equatorial oxygens. The outer set of symbols applies to the upper layer of the bilayer and the inner set to the lower layer of the bilayer. Inversion ($\mathcal{I}$) is taken with respect to the (blue) solid circle as the origin, which for bilayers is in the plane midway between the upper and lower layer. m_z is a mirror operation with respect to the plane perpendicular to the tetragonal z axis which passes through the origin.

Finally, we identify the space groups of the structures of Fig. 16. Note that $\alpha + \beta$ critical corresponds to irrep X_4^- and $\alpha - \beta$ critical corresponds to irrep X_3^- in the notation of Ref. 19. The generators of $[1\bar{1}\bar{1}1]$ are $(X \pm 1/2, Y + 1/2, Z)$,$(X, Y, Z + 1)$, $(\overline{X} + 1/2, \overline{Y}, Z)$, $(X, \overline{Y}, \overline{Z})$, and $(\overline{X}, \overline{Y}, \overline{Z})$ and those of $[\bar{1}111]$ are $(X \pm 1/2, Y + 1/2, Z)$, $(X, Y, Z + 1)$, $(\overline{X}, \overline{Y}, \overline{Z})$, $(\overline{X}, \overline{Y}, Z + 1/2)$, and $(X, \overline{Y}, \overline{Z})$. From these generators we identify the space groups as indicated in Fig. 16.

B. The star of N

Again the analysis parallels that for RP214. Now the analog of Table IV is Table VI. Here m_z has the opposite sign from Table IV. However, since the free energy contains only even powers of the ϕ variables, the free energy for the star of **N** of RP327 is the same as that for the star of **N** of RP214. In Fig. 17 we therefore show the structures in which the ϕ's for the upper layer are identical to those of the single layer in Fig. 10. Note that of all the generators of Fig. 10, only inversion $(\overline{X}, \overline{Y}, \overline{Z})$ will not be an invariant if the origins of Fig. 17 were the same as those of Fig. 10. (This is because, according to Fig. 15, inversion for $n = 2$ systems introduces an extra minus sign compared to the $n = 1$ case.) However, inversion can be made an invariant by moving the origins and this is done appropriately in Fig. 17. We thereby determine the generators to be the same as for the analogous structures in Fig. 10: For $[\bar{x}y\bar{x}\bar{y}]$ the generators are $(X + 1, Y, Z)$, $(X, Y + 1, Z)$, $(X, Y, Z + 1)$, and $(\overline{X}, \overline{Y}, \overline{Z})$, which is C_i^1 ($P\bar{1} = 2$). For both $[010\bar{1}]$ and $[\bar{1}\bar{1}\bar{1}1]$, the generators are $(X, Y, Z + 1)$, $(X + 1/2, Y + 1/2, Z)$, $(X + 1/2, Y - 1/2, Z)$, $(\overline{X}, \overline{Y}, \overline{Z})$, and $(\overline{X}, Y, \overline{Z})$, which is C_{2h}^3 ($C2/m = 12$). Although these two structures belong to the same space group, they are different because their unit cells are different (see Fig. 10).

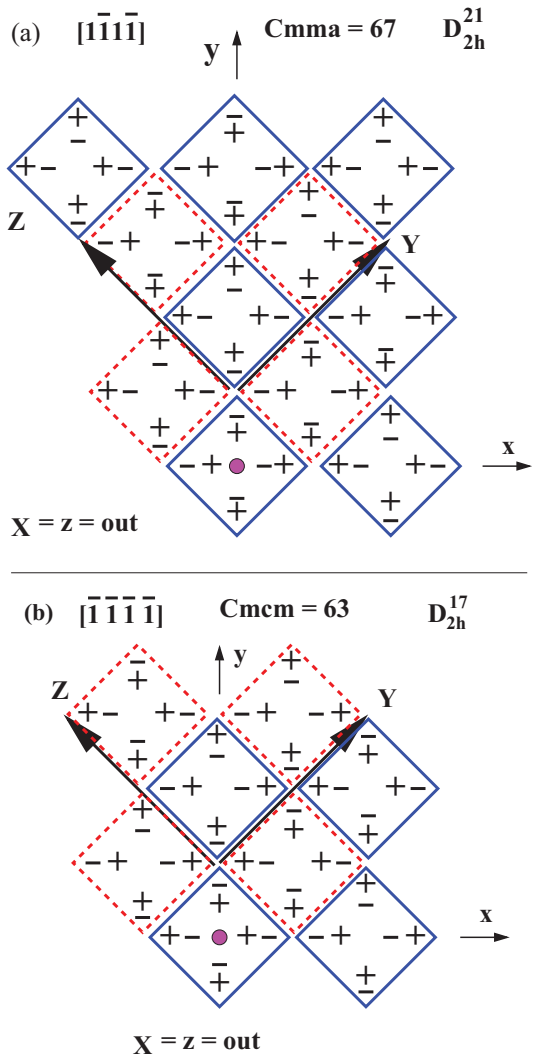

FIG. 16. (Color online) As Fig. 8 but for the star of **X** for RP327 (with invariance under $z \to z+1$). The outer + or − sign gives the sign of the z component of displacement of the upper layer of the bilayer and the inner + or − sign gives the sign of the z component of displacement of the lower layer of the bilayer. $\Psi = [1\bar{1}1\bar{1}]$ for (a) and $[\bar{1}11\bar{1}]$ for (b). The new origins are in the $z = 0$ plane (which is midway between the two layers of a bilayer). The third orthorhombic axis vector (X) is $[001]_t$.

C. The star of P

1. θ structures

The situation for θ structures at the star of **P** is similar to that at the star of **X** except that the displacements change sign under $z \to z+1$. The structures with $\theta_{n,a} = \theta_{n,b}$ have the same symmetry as that shown in Fig. 7(b): However, each single layer is replaced by a bilayer in which $\theta_{n,a} = \theta_{n,b}$. So the space group is again $I4_1/acd = 142\,(D_{4h}^{20})$. The structure with $\theta_{n,a} = -\theta_{n,b}$ and which changes sign under $z \to z+1$ is illustrated

TABLE VI. As Table I, but for the RP327 variables of the star of $\mathbf{N} \equiv (1/2,0,1/2)$ (shown in Fig. 9). $T \equiv (1/2,1/2,1/2)$, $T_x \equiv (1,0,0)$, and $T_y \equiv (0,1,0)$. All variables are odd under $\mathbf{T} \equiv (0,0,1)$.

	$\mathcal{R}_4$	m_d	m_z	T	T_x	T_y
$\phi_{x,1}$	$\phi_{y,1}$	$\phi_{y,1}$	$\phi_{x,1}$	$\phi_{x,2}$	$-\phi_{x,1}$	$\phi_{x,1}$
$\phi_{y,1}$	$-\phi_{x,1}$	$\phi_{x,1}$	$\phi_{y,1}$	$\phi_{y,2}$	$\phi_{x,1}$	$-\phi_{y,1}$
$\phi_{x,2}$	$\phi_{y,2}$	$\phi_{y,2}$	$-\phi_{x,2}$	$\phi_{x,1}$	$-\phi_{x,2}$	$\phi_{x,2}$
$\phi_{y,2}$	$\phi_{x,2}$	$\phi_{x,2}$	$-\phi_{y,2}$	$\phi_{y,1}$	$\phi_{y,2}$	$-\phi_{y,2}$

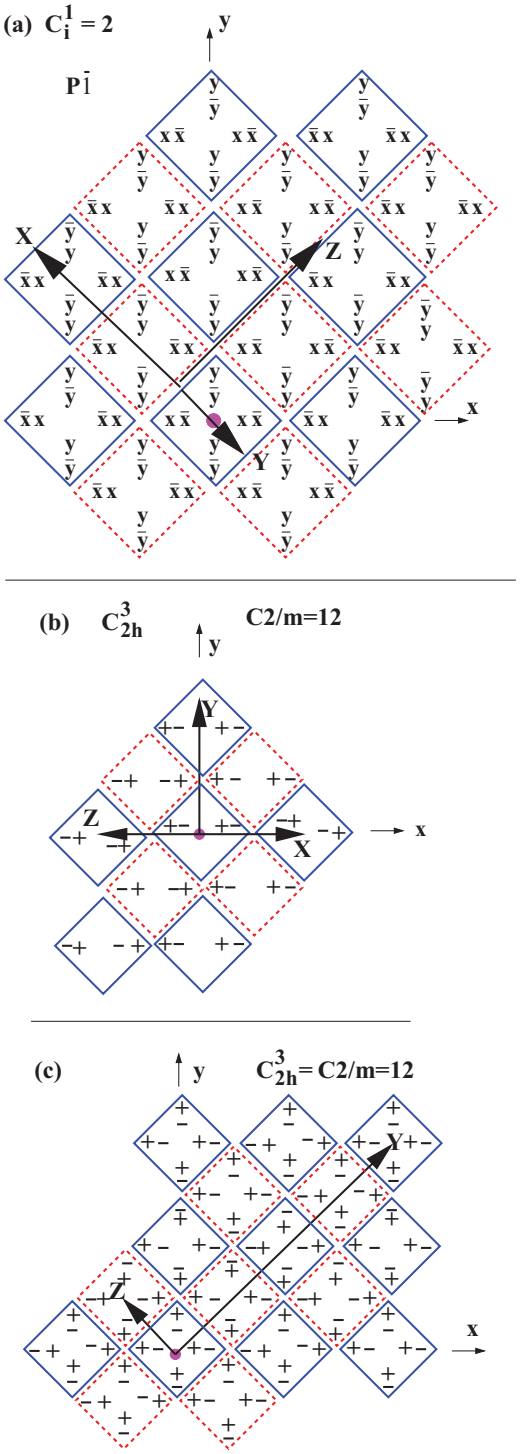

FIG. 17. (Color online) As Fig. 8 but for the star of **N** (with sign change under $z \to z+1$) for (a) $[\bar{x}y\bar{x}\bar{y}]$, (b) $[\bar{1}0\bar{1}0]$, and (c) $[\bar{1}1\bar{1}\bar{1}]$. The new axes are $X = ([\bar{1}11])$, $Y = [1/2,-1/2,1/2]$, and $Z = [1,1,\bar{1}]$ for (a), $X = [1,0,1]$, $Y = [0,1,0]$, and $Z = [\bar{1},0,1]$ for (b), and $X = [0,0,2]$, $Y = [2,2,0]$, and $Z = [-1/2,1/2,-1/2]$ for (c). The new origins are at $z = 1/4$ for (a) and at $z = 1/2$ for (b) and (c).

in Fig. 14(b). This structure is generated by $(X-1/2,Y+1/2,Z+1/2)$, $(X+1/2,Y-1/2,Z+1/2)$, $(X+1/2,Y+1/2,Z-1/2)$, $(\overline{X},\overline{Y},\overline{Z})$, $(X,\overline{Y},\overline{Z}+1/2)$, and $(\overline{Y}+1/4,X+3/4,Z+1/4)$ and is therefore $I4_1/acd = 142$ (D_{4h}^{20}). In identifying the generators we used Fig. 15.

2. ϕ structures

Again comparison of Tables I and V shows that only the only difference for ϕ variables is that m_z changes sign. However, since the free energy only involves even powers of the variables, one concludes that the free energy for the ϕ variables of the star of **P** is the same for RP327 as for RP214. Therefore, we have the structures shown in Fig. 18 where the upper layer is the same as what is shown in Fig. 11. The only difference in identifying the generators is that since inversion for RP327 differs by a sign change from that for RP214 (see Fig. 15) we had to change the sign of all the ϕ variables (in the dashed squares) for the slab at $z = 1/2$. Thus, $[\bar{1}1\bar{1}1]$ for RP214 is replaced with $[\bar{1}11\bar{1}]$ for RP327 and similarly for the other cases. We thereby identify the generators as $(X,\overline{Y},\overline{Z})$,[44] $(X,\overline{Y},\overline{Z}+1/2)$, $(\overline{X},\overline{Y},\overline{Z})$, $(X-1/2,Y+1/2,Z+1/2)$, $(X+1/2,Y-1/2,Z+1/2)$, and $(X+1/2,Y+1/2,Z-1/2)$ for (a), $(\overline{X}+1/4,\overline{Y}+1/4,Z)$, $(X,\overline{Y}+1/4,\overline{Z}+1/4)$, $(\overline{X},\overline{Y},\overline{Z})$, $(X,Y+1/2,Z+1/2)$, $(X+1/2,Y,Z+1/2)$, and $(X+1/2,Y+1/2,Z)$ for (b), and $(\overline{X},Y,\overline{Z}+1/2)$, $(\overline{X},\overline{Y},\overline{Z})$, $(X\pm1/2,Y+1/2,Z)$, and $(X,Y,Z+1)$ for (c). These lead to the space groups listed in the figure. Because of the Lifshitz instability the wave vector can be an incommensurate one close to **P** and the elastic distortion would then also be incommensurate, as is discussed in Sec. III C 2,

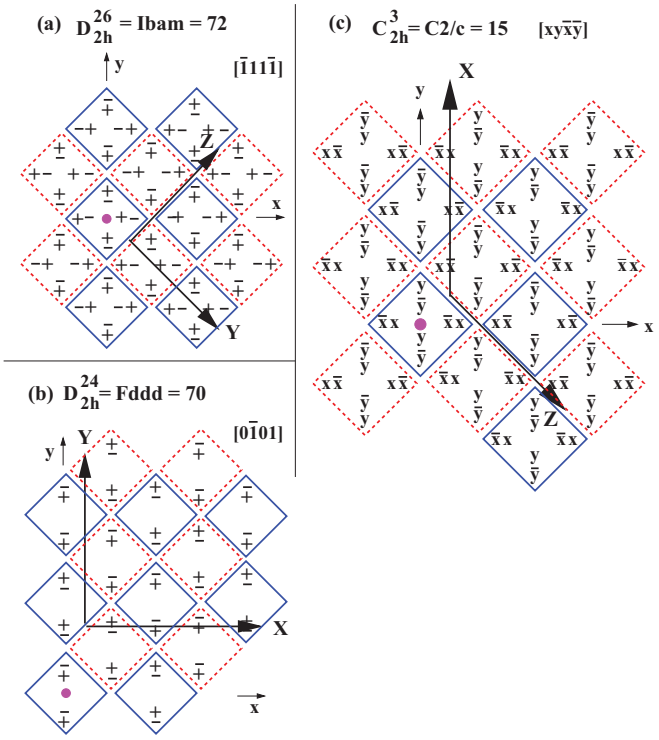

FIG. 18. (Color online) As Fig. 16 but for the star of **P** (with sign change under $z \to z+1$) for (a) $[1\bar{1}1\bar{1}]$, (b) $[0\bar{1}01]$, and (c) $[xy\bar{x}\bar{y}]$. The new out-of-plane axes are $Z = [0,0,2]$ for (a), $Y = [0,0,2]$ for (b), and $Z = [0,0,2]$ for (c). The new origins are at $z = 3/4$ in (a) and in (b) and at $z = 1/4$ in (c). The new out-of-plane axes are $(0,0,2)_t$.

V. RP SYSTEMS WITH $n > 2$

Now we are in a position to analyze the situation of RP systems with $n > 2$. For the θ structures the important issue is whether the eigenvalue $\lambda(m_z)$, which characterizes the symmetry of the stacking sequence, is $+1$ or -1. For the ϕ structures (for which ϕ is constrained to alternate in sign from one layer to the next) the important issue is, as stated in Ref. 20, whether n, the number of layers per substructure, is even or odd. So the ϕ structures for possible space groups for odd n are those given for RP214 systems and those for even n are those given for RP327 systems. In both cases the actual structures are obvious generalizations of those shown explicitly in the figures.

A. θ structures

Accordingly, we explicitly consider θ structures (see Fig. 19). The θ structures associated with the star of either **X** or **P** are governed by the free energy [when, as in Eq. (26), ϵ_{xy} is nonzero only at order λ^{-1}]

$$F = c_1\lambda\sum_{k=1}^{2}\sum_{\alpha=1}^{n}\left[\left(2\theta_{k,\alpha}^2+\epsilon_{xx}\right)^2+\left(2\theta_{k,\alpha}^2+\epsilon_{yy}\right)^2\right] + c_3\lambda\sum_{k=1}^{2}\sum_{\alpha=1}^{n}\left[\left(2\theta_{k,\alpha}^2+\epsilon_{xx}\right)\left(2\theta_{k,\alpha}^2+\epsilon_{yy}\right)\right] + \sum_{k=1}^{2}\sum_{\alpha,\beta=1}^{n}A_{\alpha,\beta}\theta_{k,\alpha}\theta_{k,\beta}+V, \tag{64}$$

where V contains interaction terms (of order λ^0) between the two different slabs. Note that quadratic terms like $\theta_{1,\alpha}\theta_{2,\beta}$ are excluded because they are not invariant under $\mathcal{R}_4$, as one sees from Table V or Fig. 12. The ordering vector of the first n-layer

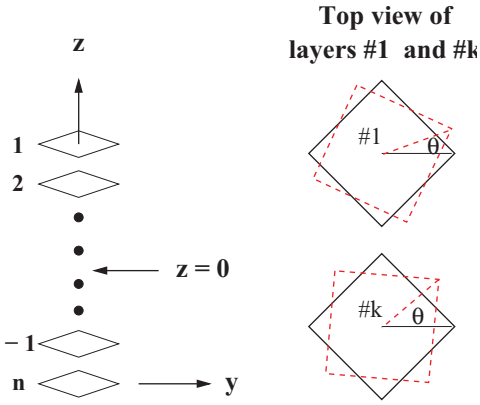

FIG. 19. (Color online) The θ structures for one of the n-layer slabs. (Left) The cross section of the n-layer slab showing the (x,y,z) coordinate system used to discuss the symmetry of the θ structures. (Right) Top view showing that the structure (red dashed cross section) is characterized by giving the value of the rotation θ for each of the n layers.

slab in the unit cell is

$$\Phi_1 = [\theta_{1,1},\theta_{1,2},\theta_{1,3},\ldots,\theta_{1,n}]. \tag{65}$$

Note that Φ is proportional to the eigenvector of the matrix **A** which has the minimal eigenvalue (so that it is the one which first becomes critical as the temperature is lowered). The matrix **A** is invariant under the mirror operation m_z which interchanges layers k and $n+1-k$, so that $\theta_k \leftrightarrow \theta_{n+1-k}$. Therefore, we know only that the eigenvector is either even or odd [i.e., the eigenvalue of m_z, $\lambda(m_z)$, is either $+1$ or -1, respectively], depending on the details of the interactions in the system. For instance, for $n=1$ $\Phi_1=[1]$ and is even under m_z. For $n=2$ the critical eigenvector is either [11] (which is even under m_z) or $[1\bar{1}]$ (which is odd under m_z). For $n=3$ the critical eigenvector is either $[10\bar{1}]$ (which is odd under m_z) or $[\alpha\beta\alpha]$, where α and β depend on the interactions within the three-layer subsystem and this eigenvector is even under m_z. On the basis of symmetry we can definitely *not* posit any specific form for the eigenvector (for $n>2$), as is done in Table XIII of Ref. 20. In all these examples the ordering vector for the second n-layer subsystem obeys $\Phi_2 = \pm\Phi_1$, where the indeterminacy in sign reflects the by now familiar frustration of θ structures.

For $n>2$ the state we call I, given by the critical eigenvector of **A**, will develop at the structural phase transition at a critical temperature we denote T_I. For this state $\theta^2_{k\alpha}$ will not be independent of k unless there is an unusual accidental degeneracy and therefore its free energy will be of the form

$$F_I = \tfrac{1}{2}(T-T_I)Q_I^2 + \alpha\lambda Q_I^4. \tag{66}$$

The quartic term must be of order λ because $\theta^2_{k,\alpha}$ is *not* independent of α. This state competes with state II which satisfies (for all k and α)

$$2\theta^2_{k\alpha} = -\epsilon_{xx} = -\epsilon_{yy}. \tag{67}$$

State I becomes critical at a temperature T_I, which is higher than that, T_{II}, at which state II becomes critical. The free energy of state II can be written as

$$F_{II} = \tfrac{1}{2}(T-T_{II})Q_{II}^2 + \beta Q_{II}^4. \tag{68}$$

Minimization with respect to the order parameters yields

$$\begin{aligned} F_I &= -\frac{1}{2}\frac{(T-T_I)^2}{\alpha\lambda}, && T<T_I,\\ F_I &= 0, && T>T_I,\\ F_{II} &= -\frac{1}{2}\frac{(T-T_{II})^2}{\beta}, && T<T_{II},\\ F_{II} &= 0, && T>T_{II} \end{aligned} \tag{69}$$

and these are plotted versus T in Fig. 20. One sees that for $n>2$ we have a more complicated phase diagram than for $n=1$ or 2. When λ is large, for a small range of temperature phase I is stable, but at lower T we arrive at phase II. For $n>3$ it is possible to have more than one phase transition before ultimately reaching phase II.

The possible θ structures of phase I depend on the wave vector (**X** or **P**) and whether the interactions within the system select $\lambda(m_z)=+1$ or -1. First consider the star of **X**, for which $\theta(z+1)=\theta(z)$. If $\lambda(m_z)=+1$ [as in Fig. 7(a)], then, irrespective of the value of the number of layers per slab n, we will have a structure similar to that of Fig. 7(a) (in which each layer of Fig. 7 is replaced by an n-layer slab) with space group $Cmca=64$. If interactions select, $\lambda(m_z)=-1$ (this is only possible for $n>1$), then we have a structure of space group $Ccca=68$, similar to that shown in Fig. 14(a). Next consider the star of **P**, for which $\theta(z+1)=-\theta(z)$. If $\lambda(m_z)=+1$ [as in Fig. 7(b)], then, irrespective of the value of the number of layers per slab n, we will have a structure similar to that of Fig. 7(b) with space group $I4_1/acd=142$. If interactions select $\lambda(m_z)=-1$ (this is only possible for $n>1$), then we have a structure of space group $I4_1/acd=142$, similar to that shown in Fig. 14(b).

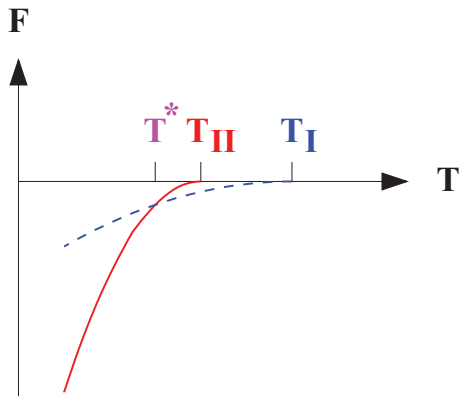

FIG. 20. (Color online) The free energies of phase I (dashed line) and phase II (solid line), as given by Eq. (69). These curves are drawn for $\xi \equiv \alpha\lambda/\beta = 9$. Phase I is stable for $T^* < T < T_I$. From Eq. (69) the I $\rightarrow$ II phase transition occurs at $T^* = T_{II} - (T_I - T_{II})/(\sqrt{\xi}-1)$.

The above remarks relied only on symmetry. However, now we consider the likely form of the interaction matrix $A_{\alpha\beta}$ in Eq. (64), which determines θ as a function of the layer index α. If the dominant intraslab interactions are those between adjacent layers, then, as illustrated in Fig. 21, we obtain configurations analogous to ferromagnetic [panels (a) and (c)] or antiferromagnetic [panels (b) and (d)] spin structures. Thus, with nearest-neighbor interlayer interactions, if n, the number of layers per slab is even, we can have either sign of $\lambda(m_z)$. If n is odd, then this special ansatz of nearest-neighbor interlayer interactions can only give $\lambda(m_z)=+1$. If, experimentally, the case $\lambda(m_z)=-1$ is observed for odd n, one could conclude the existence of significant longer range interlayer interactions. (Such a situation is obviously possible in the presence of Coulomb interactions.)

Our results are summarized in Table VII. Note that for the θ structures the controlling variable is not the number of layers n, but $\lambda(m_z)$. It is interesting to note that for **N** and **P**, the ϕ structures for even and odd $\lambda(m_z)$ are very similar, as one can see by comparing Figs. 10 and 17 for **N** and Figs. 11 and 18 for **P**.

We have already compared our results with those of Ref. 17. Now we compare our results for general n with those of Table XIII of Ref. 20, where it seems that only results for the star of **X** are given. One sees that of the 12 structures (2–13), only 2, 5, 9, and 12 have the same distortions in both slabs and are therefore the only structures allowed by our analysis. In that reference the distinction is made between the cases of even and odd values of n, the number of layers per slab. If one assumes

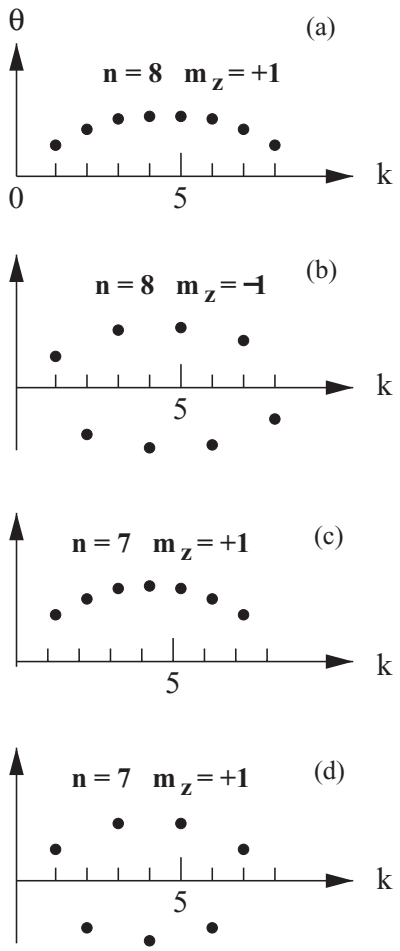

FIG. 21. Typical variation of θ as a function of the layer index, k, for dominant nearest-neighbor interlayer interaction, $A_{k,k+1} \equiv w$. For case (a), n is even and $w < 0$, so that $\lambda(m_z) = +1$. For case (b), n is even and $w > 0$, so that $\lambda(m_z) = -1$. For cases (c) and (d) n is odd. For case (c) $w < 0$ and for case (d) $w > 0$. In both cases $\lambda(m_z) = +1$. (m_z takes k into $8 - k$.) To obtain $\lambda(m_z) = -1$ for n odd requires further neighbor interlayer interactions.

(incorrectly; see Fig. 21) that $|\theta|$ is constant within a slab, then the results of Table XIII of Ref. 20 for the allowed structures are equivalent to ours. However, it is more accurate to classify the distortions according to their mirror symmetry as is done here.

VI. DISCUSSION AND CONCLUSION

We did not deal with the positions of the ions at the center of the octahedra or those between the layers of octahedra. Here we are concerned only with such ionic positions as they are modified by the orientational structural transition. Each such ion sits in a stable potential well. The question is whether or not for systems without any accidental degeneracy there is a bifurcation so that additional space groups could be allowed when the positions of these "inessential" ions are taken into account. The stable potential well can be distorted and the placement of its minimum will be modified by the octahedral reorientation. However, a single minimum of a stable potential well cannot be continuously deformed into a double well without assuming an accidental vanishing of the fourth-order term in the local potential. Similar arguments show that the perturbative effect of the center-of-mass coordinates of the nearly rigid octahedra do not produce anomalous effects.[45] Of course, parameters of Wykoff orbits which are not fixed by symmetry will be perturbatively modified at the structural phase transition. As we have discussed for several cases, elastic strains will be induced consistent with the symmetry of the distorted phase.

Experimentally, it is striking that the structures observed as distortions from the tetragonal phase are in our much shorter list. For instance, in the data cited on p. 313 and following of Ref. 20 five systems with ϕ tilts are shown which go into either $Cmca$ (64) or $P4_2/ncm$ (138), except for Rb_2CdCl_4 whose structure is uncertain: either $Cmca$ or $Fccm$ (which is on neither our list nor that of Ref. 17 because it involves two irreps). Systems (other than Rb_2CdCl_4 subsequently discussed in Ref. 20) in Table III of Ref. 17 likewise go into either $Cmca$ or $P4_2/ncm$.

To summarize, we have analyzed the possible structural transitions of the so-called RP perovskite structure (such as K_2MnF_4 or $Ca_3Mn_2O_7$, etc.) using a variant of Landau theory in which the constraint of rigid oxygen octahedra is implemented and our results are compared to the well-known results of Refs. 17 and 20. A check on the accuracy of our treatment of symmetry is that our list of allowed structures (for K_2MgF_4) which can be reached via a single structural phase transition is a *subset* of the list of Ref. 17. We find that the rigid octahedral constraint eliminates most of the structures in Table I of Ref. 17 for which the octahedral tilting transitions are discontinuous. It is also appealing that structures which are allowed by symmetry but which involve the simultaneous existence of distorted and undistorted sublattices are eliminated by the octahedral constraint. The results for the K_2MgF_4 structure are summarized in Tables II and III, where one sees that our analysis allows only 10 of the 41 structures listed in Ref. 17. A summary of our results for commensurate structures for $A_{n+1}B_nC_{3n+1}$ is given in Table VII. There one sees that if we restrict attention to continuous transitions into a commensurate structure (thus not allowing N or L in the last column), there are then only four possible structures for $n = 1$ and six possible structures for $n > 1$. (If one further restricts interlayer interactions to be only those between adjacent layers, then when n is odd one has only four possible structures.) The extension of the present analysis to treat structures reached by two phase transitions (so that they are described by two distinct irreps) will be published separately.

ACKNOWLEDGMENTS

I am grateful to T. Yildirim for performing the first principles calculations. I thank J. M. Perez-Mato, C. J. Fennie, B. Campbell, and H. T. Stokes for helpful discussions. I also thank T. C. Lubensky for calling my attention to the importance of thermal fluctuations for the elastic constants.

APPENDIX A: ANISOTROPY

Here we show that the direction in order parameter space which minimizes the free energy at order λ is stable when

TABLE VII. Summary of results for commensurate structures for RP n layer systems. $\vec{Q}$ denotes the wave vector, Var labels the angular variable, and λ is the eigenvalue of the mirror operation within the n-layer substructure, as discussed below Eq. (65). In the last column we indicate whether the transition is allowed to be continuous (Y) or not (N) or whether there is a Lifshitz instability (L). The transitions to the $C2/m$ structure are fluctuation induced first order ones. See Table I of Ref. 19.

$\vec{Q}$	Var.	λ	Space group(s)	n	See Fig.	Y,N,L
X	θ	-1	68 (D_{2h}^{22}) $Ccca$	$n > 1$[a]	14(a)	Y
X	θ	$+1$	64 (D_{2h}^{18}) $Cmca$	$n \geqslant 1$	7(a)	Y
P	θ	-1	142 (D_{4h}^{20}) $I4_1/acd$	$n > 1$[a]	14(b)	Y
P	θ	$+1$	142 (D_{4h}^{20}) $I4_1/acd$	$n \geqslant 1$	7(b)	Y
X	ϕ	$+1$	64 (D_{2h}^{18}) $Cmca$	Odd	8(a)	Y
			66 (D_{2h}^{20}) $Cccm$	Odd	8(b)	Y
X	ϕ	-1	63 (D_{2h}^{17}) $Cmcm$	Even	16(b)	Y
			67 (D_{2h}^{21}) $Cmma$	Even	16(a)	Y
N	ϕ	$+1$	12 (C_{2h}^{3}) $C2/m$	Odd	10(b)	N
			12 (C_{2h}^{3}) $C2/m$	Odd	10(c)	N
			2 (C_{i}^{1}) $P\bar{1}$	Odd	10(a)	N
N	ϕ	-1	12 (C_{2h}^{3}) $C2/m$	Even	17(b)	N
			12 (C_{2h}^{3}) $C2/m$	Even	17(c)	N
			2 (C_{i}^{1}) $P\bar{1}$	Even	17(a)	N
P	ϕ	$+1$	72 (D_{2h}^{26}) $Ibam$	Odd	11(a)	L
			70 (D_{2h}^{24}) $Fddd$	Odd	11(b)	L
			15 (C_{2h}^{3}) $C2/c$	Odd	11(c)	L
P	ϕ	-1	72 (D_{2h}^{26}) $Ibam$	Even	18(a)	L
			70 (D_{2h}^{24}) $Fddd$	Even	18(b)	L
			15 (C_{2h}^{3}) $C2/c$	Even	18(c)	L

[a]If the dominant interlayer interactions are those between adjacent layers, then, as discussed in the text, n must be even for this case to occur.

perturbations at order λ^0 are considered. For this purpose we need to show that the gradient of the terms of lower order in λ in order parameter space vanish at the minimum determined by the terms of order λ. If this were not the case, then the symmetry could be lowered by inclusion of terms of lower order in λ.

1. θ variables at the star of X

We are interested in the situation near the minimum of the free energy for large λ given by Eq. (27), so that $\theta_2 = \sigma\theta_1$, where $\sigma = \pm 1$. There are two cases depending on the sign of σ. When $\sigma = 1$ we set $\theta_1 = \theta + \epsilon$ and $\theta_2 = \theta - \epsilon$. Table I indicates that the operator T interchanges θ_1 and θ_2, or, in other words, that $T\epsilon = -\epsilon$. This indicates that

$$\partial F/\partial\epsilon|_{\epsilon=0} = 0, \tag{A1}$$

which is what we needed to establish. When $\sigma = -1$ we set $\theta_1 = \theta + \epsilon$ and $\theta_2 = -\theta + \epsilon$. Then Table I gives that $T(\theta + \epsilon, -\theta + \epsilon) = (-\theta + \epsilon, \theta + \epsilon)$ and further that $T_x T = (\theta - \epsilon, -\theta - \epsilon)$, so that again we conclude that $T_x T\epsilon = -\epsilon$ and thus that $\partial F/\partial\epsilon|_{\epsilon=0} = 0$. Therefore, the minimum of Eq. (27) for large λ is stable against inclusion of corrections at lower order in λ.

2. ϕ variables at the star of X

We perform a similar analysis for the ϕ variables of the star of **X**. We consider the critical channels for $\sigma = \pm 1$, such that

$$\phi_{x,1} = \sigma\phi_{y,2}, \qquad \phi_{x,2} = \sigma\phi_{y,1}. \tag{A2}$$

These relations are exact for the critical channels. We want to study deviations from the anisotropy at large λ, where

$$\phi_{x,1} \approx \eta\phi_{x,2}, \qquad \phi_{y,1} \approx \eta\phi_{y,2}, \tag{A3}$$

with $\eta = \pm 1$. So we have four cases depending on the signs of σ and η. In accord with these relations we consider the wave function

$$\begin{aligned}\Psi &\equiv [\phi_{x,1}, \phi_{y,1}, \phi_{x,2}, \phi_{y,2}] \\ &= [\alpha + \epsilon, \sigma\eta(\alpha - \epsilon), \eta(\alpha - \epsilon), \sigma(\alpha + \epsilon)].\end{aligned} \tag{A4}$$

We want to show that $\partial F/\partial\epsilon)_{\epsilon=0} = 0$ which follows from

$$F(\epsilon) = F(-\epsilon). \tag{A5}$$

We show in Table VIII the effect of the operators T and T_x on Ψ. For $\eta = +1$ and $\sigma = \pm 1$, we see that $T\Psi(\epsilon) = \Psi(-\epsilon)$, which verifies Eq. (A5). For $\eta = -1$ and $\sigma = \pm 1$, we see that $T_x T\Psi(\epsilon) = \Psi(-\epsilon)$, which verifies Eq. (A5). Therefore, for all four cases we have established Eq. (A1) which guarantees

TABLE VIII. Ψ of Eq. (A4) for the star of **X**, $T\Psi$ and $T_x\Psi$, where the operators T and T_x are defined in Table I. σ and η are either $+1$ or -1.

	$\phi_{x,1}$	$\phi_{y,1}$	$\phi_{x,2}$	$\phi_{y,2}$
$\Psi =$	$\alpha+\epsilon$	$\sigma\eta(\alpha-\epsilon)$	$\eta(\alpha-\epsilon)$	$\sigma(\alpha+\epsilon)$
$T\Psi =$	$\eta(\alpha-\epsilon)$	$\sigma(\alpha+\epsilon)$	$(\alpha+\epsilon)$	$\sigma\eta(\alpha-\epsilon)$
$T_xT\Psi =$	$-\eta(\alpha-\epsilon)$	$\sigma(\alpha+\epsilon)$	$-(\alpha+\epsilon)$	$\sigma\eta(\alpha+\epsilon)$

that the location of the minimum for large λ is not modified by correction terms.

3. ϕ variables at the star of N

Since we are studying the status of the relations of Eq. (40) we set

$$\begin{aligned}\Psi &= [\phi_{x,1},\phi_{y,1},\phi_{x,2},\phi_{y,2}]\\ &= [\alpha+\epsilon,\beta+\delta,\sigma(\alpha-\epsilon),\eta(\beta-\delta)].\end{aligned}\tag{A6}$$

To show that the minima for $\delta=\epsilon=0$ are stable we need to show that

$$|\partial F/\partial\delta|_{\delta=\epsilon=0} = |\partial F/\partial\epsilon|_{\delta=\epsilon=0} = 0.\tag{A7}$$

We do that by showing that the free energy is invariant under $(\epsilon,\delta)\to(-\epsilon,-\delta)$. We show in Table IX the symmetry properties of the wave functions for the star of **N**. Note that there are four cases depending on the signs of σ and η. For $\sigma=\eta=+1$, we have that $T\Psi(\epsilon,\delta)=\Psi(-\epsilon,-\delta)$, which guarantees that F is an even function of these variables. For $\sigma=-\eta=1$, we have that $T_yT\Psi(\epsilon,\delta)=\Psi(-\epsilon,-\delta)$, which guarantees that F is an even function of these variables. For $\sigma=-\eta=-1$, we have that $T_xT\Psi(\epsilon,\delta)=\Psi(-\epsilon,-\delta)$, which guarantees that F is an even function of these variables. Finally, for $\sigma=\eta=-1$, we have that $T_xT_yT\Psi(\epsilon,\delta)=\Psi(-\epsilon,-\delta)$, which guarantees that F is an even function of these variables. Thus, we have shown that at all of equivalent minima the gradients vanish, so that these minima are stable with respect to perturbations at lower order in λ.

APPENDIX B: QUALITATIVE DISCUSSION OF THE ELASTIC RESPONSE

Here I discuss *qualitatively* the role of thermal fluctuations. For the main issue of this paper, that is, the symmetry analysis of allowable phase transitions our mean-field treatment of interlocking octahedra is appropriate. However, if one wishes to discuss the elastic response, the mean-field treatment is insufficient and it would be incorrect to interpret the results of Eq. (19) as reasonable approximations to the elastic constants.

TABLE IX. As Table VIII, but for the star of **N**.

	$\phi_{x,1}$	$\phi_{y,1}$	$\phi_{x,2}$	$\phi_{y,2}$
$\Psi =$	$\alpha+\epsilon$	$\beta+\delta$	$\sigma(\alpha-\epsilon)$	$\eta(\beta-\delta)$
$T\Psi =$	$\sigma(\alpha-\epsilon)$	$\eta(\beta-\delta)$	$(\alpha+\epsilon)$	$\beta+\delta$
$T_xT\Psi =$	$-\sigma(\alpha-\epsilon)$	$\eta(\beta-\delta)$	$-(\alpha+\epsilon)$	$\beta+\delta$
$T_yT\Psi =$	$\sigma(\alpha-\epsilon)$	$-\eta(\beta-\delta)$	$(\alpha+\epsilon)$	$-(\beta+\delta)$
$T_xT_yT\Psi =$	$-\sigma(\alpha-\epsilon)$	$-\eta(\beta-\delta)$	$-(\alpha+\epsilon)$	$-(\beta+\delta)$

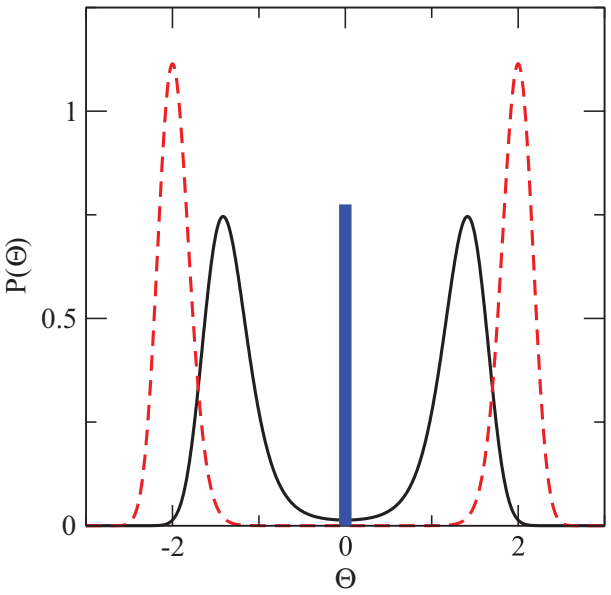

FIG. 22. (Color online) The single octahedron rotational angle (θ) probability distribution function $P(\theta)$ in the high symmetry phase. The solid (black) line is for the unstressed system and the dashed (red) line is for the system under compressional stress. For comparison we also indicate (in blue) the delta-function distribution implied by mean-field theory.

These elastic constants would be proportional to $\lambda\gg 1$ if compression or elongation were performed while keeping the octahedra perfectly aligned. However, it is clear that the octahedra will rotate to relieve any applied stress, σ. This is clear when the stress involves compression ($\sigma>0$). Under extension, it is essential to treat the equilibrium phase as one in which the octahedral orientations are subject to a distribution function (see Fig. 22), so that in the generic situation the octahedra are not perfectly aligned.

The canonical approach to include fluctuations would be to integrate out of the partition function the fluctuations about the mean-field state. For instance, if a fluctuation is considered to be an oscillator having frequency ω, then its contribution to the free energy is of order $kT\ln(\hbar\omega/kT)$. This energy can be relevant if the elastic modes have a much higher energy (as they do) for perfectly aligned octahedra than for tilted octahedra. Because this thermal fluctuation free energy is much higher when the octahedra are perfectly aligned, it favors having the tilting angle θ be nonzero. Of course, this mechanism does not favor one sign or the other for θ. It does suggest that the system will form regions having different signs of θ giving rise to a probability distribution for θ as shown in Fig. 22. Thus, the structural transformation is probably similar to an order-disorder transition of an Ising model. However, at temperatures slightly above the structural phase transition the system consists of regions having $\theta\approx\pm\theta_0$. As shown in Fig. 22, the value of θ_0 responds to applied stress σ with $d\theta_0/d\sigma>0$. Note that this picture does not imply that the symmetry of the system with thermal fluctuations is any different from that without such fluctuations. So this picture only serves to explain that one should not use the calculations of this paper to make statements about the magnitude of the elastic constants.

Since the energy of domain walls competes with the energy needed to deform the octahedra it is likely that $C_{11} \sim \lambda^x$, with $x < 1$. If the analogy with magnetic domain walls[46] is applicable, then perhaps $x = 1/2$.

*harris@sas.upenn.edu

[1] S. N. Ruddlesden and P. Popper, Acta Crystallogr. **11**, 54 (1958).

[2] J. D. Bednorz and K. A. Müller, Z. Phys. B **64**, 189 (1986).

[3] Y. Tokura (editor), *Colossal Magnetoresistance Oxides*, monograph in Condensed Matter Science (Gordon and Breach, London, 2000).

[4] J. F. Mitchell, D. N. Argyriou, A. Burger, K. E. Grey, R. Osborn, and U. Welp, J. Phys. Chem. B **105**, 10732 (2001).

[5] M. V. Lobanov, M. Greenblatt, El'ad N. Caspi, J. D. Jorgensen, D. V. Sheptyakov, B. H. Toby, C. E. Botez, and P. W. Stephens, J. Phys.: Condens. Matter **16**, 5339 (2004).

[6] N. A. Benedek and C. J. Fennie, Phys. Rev. Lett. **106**, 107204 (2011).

[7] A. B. Harris, Phys. Rev. B **84**, 064116 (2011).

[8] K. R. Poepplemeier, M. E. Leonowicz, J. C. Scanlon, J. M. Longo, and W. B. Yelon, J. Solid State Chem. **45**, 71 (1982).

[9] M. E. Leonowicz, K. R. Poepplemeier, and J. M. Longo, J. Solid State Chem. **71**, 59 (1985).

[10] P. D. Battle, M. A. Green, N. S. Laskey, J. E. Millburn, L. Murphy, M. J. Rosseinsky, S. P. Sullivan, and J. F. Vente, Solid State Chem. **59**, 71 (1995).

[11] P. D. Battle, M. A. Green, J. Lago, J. E. Millburn, M. J. Rosseinsky, and J. F. Vente, Chem. Mater. **10**, 658 (1998).

[12] I. D. Fawcett, J. E. Sunstrom IV, M. Greenblatt, M. Croft, and K. V. Ramanujachary, Chem. Mater. **10**, 3643 (1998).

[13] Th. Hahn (editor) *International Tables for Crystallography* (Kluwer Academic, Dordrecht, 1995), Vol. A.

[14] A. M. Glazer, Acta Crystallogr. Sect. B **28**, 3384 (1972).

[15] P. M. Woodward, Acta Crystallogr. Sect. B **53**, 32 (1997).

[16] K. S. Aleksandrov, B. V. Beznosikov, and S. V. Misyul, Phys. Status Solidi A **104**, 529 (1987).

[17] D. M. Hatch, H. T. Stokes, K. S. Aleksandrov, and S. V. Misyul, Phys. Rev. B **39**, 9282 (1989).

[18] ISODISTORT (accessible from the internet).

[19] H. T. Stokes and D. M. Hatch, *Isotropy Subgroups of the 230 Crystallographic Space Groups* (World-Scientific, Singapore, 1988).

[20] K. S. Aleksandrov and J. Bartolomé, Phase Transitions **74**, 255 (2001).

[21] K. S. Aleksandrov and J. Bartolomé, J. Phys.: Condens. Matter **6**, 8219 (1994).

[22] A. summary of relevant data for pseudocubic perovskites is given by J.-S. Zhou and J. B. Goodenough, Phys. Rev. B **77**, 132104 (2008).

[23] See p. 3385 of Ref. 14.

[24] A. B. Harris, e-print arXiv:1012.5127.

[25] Lengths are in units of lattice constants a_i and wave vectors in units of $2\pi/a_i$.

[26] See Wikipedia entry for "Multicritical point."

[27] A. D. Bruce and A. Aharony, Phys. Rev. B **11**, 478 (1975).

[28] Since we focus on the displacements of ions, we denote the displacements as θ and ϕ_α rather than $a\theta/2$ and $a\phi_\alpha/2$, as we would if θ and ϕ_α were the angle variables.

[29] A criticism taken from a referee report of e-print arXiv:1012.5127.

[30] J. M. Perez-Mato, M. Aroyo, A. Garcia, P. Blaha, K. Schwarz, J. Schweifer, and K. Parlinski, Phys. Rev. B **70**, 214111 (2004).

[31] J. López-Perez and J. Íñiguez, Phys. Rev. B **84**, 075121 (2011).

[32] T. Yildirim (to be published).

[33] It may be easy to overlook this simple relationship for inversion symmetry: According to Referee C of e-print arXiv:1012.5127, ". . . the inversion about the origin is . . . not present in Table I among the other generators." A count of symmetry operations, 4 for $\mathcal{R}_4$, 2 for m_d, and 2 for m_z, indicates that Table I does include all 16 operations of the point group, including inversion about the origin.

[34] Our notation is such that (X', Y', Z') denotes the operation which takes (X, Y, Z) into (X', Y', Z'). Thus, $\mathcal{R}_4 = (-Y, X, Z)$.

[35] See Table 2 of Ref. 19 for a convenient listing of the generators of each space group.

[36] W. Press, J. Chem. Phys. **56**, 2597 (1972).

[37] E. F. Shender, Zh. Eksp. Teor. Fiz. **83**, 326 (1982) [Sov. Phys. JETP **56**, 178 (1982)].

[38] T. Yildirim, A. B. Harris, and E. F. Shender, Phys. Rev. B **53**, 6455 (1996).

[39] C. P. Bean and D. S. Rodbell, Phys. Rev. **126**, 104 (1962).

[40] D. J. Bergmann and B. I. Halperin, Phys. Rev. B **13**, 2145 (1976).

[41] Equivalent structures are those related by rotations and translations. Structures related only by improper rotations (this includes mirrors) may be enantiomorphs and may be from distinct space groups. So here and below we prefer to not invoke improper rotations to test for equivalence.

[42] Note: Here and below [except in panel (b) of Fig. 18, where we make a more convenient choice of axes] we choose the representative to reproduce the setting chosen in Refs. 17 and 19.

[43] Y. Onodera and Y. Tanabe, J. Phys. Soc. Jpn. **45**, 1111 (1978).

[44] It is more convenient to replace $(\overline{x}, \overline{y}, z)$ in the set of generators of $Ibam$ given in Ref. 19 with $(x, y, \overline{z})$.

[45] We do not treat the symmetry-breaking displacements of the B ions away from the center of the octahedra.

[46] C. Kittel, Rev. Mod. Phys. **21**, 541 (1949).